



Functional Hyperspectral Imaging by High-Related Vegetation Indices to Track the Wide-Spectrum *Trichoderma* Biocontrol Activity Against Soil-Borne Diseases of Baby-Leaf Vegetables

Gelsomina Manganiello, Nicola Nicastro, Michele Caputo, Massimo Zaccardelli, Teodoro Cardì and Catello Pane*

Consiglio per la ricerca in agricoltura e l'analisi dell'economia agraria, Centro di ricerca Orticoltura e Florovivaismo, Pontecagnano Faiano, Italy

OPEN ACCESS

Edited by:

Qingguo Xie,
Huazhong University of Science and
Technology, China

Reviewed by:

Michael Gomez Selvaraj,
Consultative Group on International
Agricultural Research (CGIAR),
United States
Omar Vergara-Diaz,
University of Barcelona, Spain

*Correspondence:

Catello Pane
catello.pane@crea.gov.it

Specialty section:

This article was submitted to
Technical Advances in Plant Science,
a section of the journal
Frontiers in Plant Science

Received: 19 November 2020

Accepted: 28 January 2021

Published: 24 February 2021

Citation:

Manganiello G, Nicastro N, Caputo M,
Zaccardelli M, Cardì T and Pane C
(2021) Functional Hyperspectral
Imaging by High-Related Vegetation
Indices to Track the Wide-Spectrum
Trichoderma Biocontrol Activity
Against Soil-Borne Diseases of
Baby-Leaf Vegetables.
Front. Plant Sci. 12:630059.
doi: 10.3389/fpls.2021.630059

Research has been increasingly focusing on the selection of novel and effective biological control agents (BCAs) against soil-borne plant pathogens. The large-scale application of BCAs requires fast and robust screening methods for the evaluation of the efficacy of high numbers of candidates. In this context, the digital technologies can be applied not only for early disease detection but also for rapid performance analyses of BCAs. The present study investigates the ability of different *Trichoderma* spp. to contain the development of main baby-leaf vegetable pathogens and applies functional plant imaging to select the best performing antagonists against multiple pathosystems. Specifically, sixteen different *Trichoderma* spp. strains were characterized both *in vivo* and *in vitro* for their ability to contain *R. solani*, *S. sclerotiorum* and *S. rolfsii* development. All *Trichoderma* spp. showed, *in vitro* significant radial growth inhibition of the target phytopathogens. Furthermore, biocontrol trials were performed on wild rocket, green and red baby lettuces infected, respectively, with *R. solani*, *S. sclerotiorum* and *S. rolfsii*. The plant status was monitored by using hyperspectral imaging. Two strains, T135 and Ta56, belonging to *T. longibrachiatum* and *T. atroviride* species, significantly reduced disease incidence and severity (DI and DSI) in the three pathosystems. Vegetation indices, calculated on the hyperspectral data extracted from the images of plant-*Trichoderma*-pathogen interaction, proved to be suitable to refer about the plant health status. Four of them (OSAVI, SAVI, TSAVI and TVI) were found informative for all the pathosystems analyzed, resulting closely correlated to DSI according to significant changes in the spectral signatures among health, infected and bio-protected plants. Findings clearly indicate the possibility to promote sustainable disease management of crops by applying digital plant imaging as large-scale screening method of BCAs' effectiveness and precision biological control support.

Keywords: BCAs, *Sclerotinia sclerotiorum*, *Sclerotium rolfsii*, *Rhizoctonia solani*, *Diplotaxis tenuifolia*, *Lactuca sativa*, fresh-cutting vegetables, plant reflectance

INTRODUCTION

Baby leaf vegetables constitute the major ingredient of ready-to-eat salads, very appreciated worldwide by consumers looking for healthy diets rich in fibers and low in calories, with organoleptic and nutraceutical traits particularly enhanced in pigmented varieties. Currently, in Italy, which is among the top European producers of these crops, it is estimated that more than 4,500 hectares are devoted, both in tunnels and, marginally, in open field, to grow baby salads for the high convenience food chain (Morra et al., 2017). A rather large group of different leafy vegetable species are included under this appellation, although by far, wild rocket [*Diplotaxis tenuifolia* (L.) DC.] and baby lettuce (*Lactuca sativa* L. var. *acephala*) are the most extensively cultivated. Because of the intensive exploitation of soils, continuous cropping, cultivars susceptibility to pathogens and reduced use of synthetic fungicides, those crops are dramatically prone to several diseases occurring in the humid and temperate microclimate of the sprinkler-irrigated tunnels/fields (Caruso et al., 2018; Gilardi et al., 2018a,b; Gullino et al., 2019). The soil-borne fungi *Rhizoctonia solani* Kuhn, *Sclerotinia sclerotiorum* (Lib.) de Bary and *Sclerotium rolfsii* Sacc., belonging to the *Phylum* Basidiomycota, are parenchymatic, polyphagous, necrotrophic pathogens of different salad crops, causing huge economic losses and symptoms ranging from the simple rotting of the attacked organs to the damping-off. Their non-chemical counteraction is particularly requested under sustainable management systems pursuing the zero residues goal, while it is mandatory according to the organic farming rules (Giménez et al., 2019). To this scope, the integrated disease management people are exploring alternative approaches to synthetic fungicides, including the implementation of effective microbes able to control phytopathogenic attacks, referred as biological control agents (BCAs).

Soil microbiota represents a precious reservoir of biocontrol microorganisms to impact plant health, growth and productivity in agricultural applications. Several fungal species belonging to the genus *Trichoderma* (Ascomycota) are known to suppress soil-borne and foliar plant diseases directly by mechanisms against the host pathogen (competition for space and nutrients, antibiosis, and mycoparasitism) and indirectly by the induction of a resistance responses in the colonized plants (Howell, 2003). Because of their crucial role as antagonists, *Trichoderma* spp. are among the most effective and commercialized biological control agents, registered as Plant Protection Products to manage a broad-spectrum of plant pathogens (Sharma et al., 2019). A number of *Trichoderma* spp. antagonistic strains are sourced from several telluric environments carrying disease control-related functions, including suppressive composts, to gain increasing efficacy firstly due to the niche-competence shared with the targeted soil-borne pathogens (Wang et al., 2019). The selection of novel and effective BCAs requires fast and robust screening methods suitable to evaluate high numbers of candidates. In this context, digital technologies, such as remote sensing, could play a pivotal role not only for early disease detection but also for the rapid performance analyses of BCAs and in the prediction of the biocontrol efficacy.

Hyperspectral imaging is a non-destructive and powerful digital technology to directly identifying biochemical and physiological shifts occurring in plants in response to external stimuli, including pathological prodding (Thomas et al., 2018). It involves the pixel-by-pixel analysis of an image containing spatially distributed the reflectance spectrum captured in the visible (VIS, spectral range 400–700 nm) and near infrared (NIR 700–1,000 nm) regions as hypercube dataset resulting by the interaction of the canopy with the incident light (Liu H. et al., 2020). Several previous hyperspectral studies pointed up broad/narrow extracted band indices, called vegetation indices (VIs) that have been used to associate the spectral information to several crop characteristics (Thenkabail et al., 2000), including plant health (Xue and Su, 2017). For example, the best known one, Normalized Difference Vegetation Index (NDVI) that is predictive of the vegetative growth and the general plant status (Rouse et al., 1973), recently was also proposed to refer about the *Vitis vinifera* – *Botrytis cinerea* interaction (Pañitru-De la Fuente et al., 2020). The sensitivity of hyperspectral VIs about disease grade of the canopy, was also proposed to automatically evaluate the performances of disease control methods as innovative functional application (Martins et al., 2018). In this view, hyperspectral imaging may additionally help the fine scouting of new effective microbial antagonists under selection by configuring a standard quantitative analytic method to follow biocontrol dynamics that can be usefully implemented in a perspective definition of precision biological control guidelines.

The aim of this work was to select new useful antagonistic strains of *Trichoderma* able to protect wild rocket and baby lettuce from deleterious soil-borne pathogens. *R. solani* and *S. sclerotiorum* infections are very diffuse among these cultivations while *S. rolfsii* is going emerging importance on baby-leaf because of its attitude to grow at high temperature regime, as under greenhouse. Additionally, computing the reflectance data from the canopy of the bio-treated plants, this study can lead to the identification of high-performing vegetative indices (VIs) functional to the large-scale evaluation of the biocontrol effectiveness and, furthermore, to discriminate between healthy and infected plants.

MATERIALS AND METHODS

Isolation of *Trichoderma* Strains

The sixteen *Trichoderma* strains characterized here, were isolated from a high suppressive rocket and fennel-derived compost (Pane et al., 2020; Scotti et al., 2020) and stored in the fungal collection of CREA-Centro di ricerca Orticoltura e Florovivaismo (Pontecagnano Faiano, Italy CREA-OF). Isolates were subjected to monosporic culturing by serial ten-fold dilution. For the strain characterization, macroscopic features (medium pigmentation, colony color, colony edge shape, smell) were evaluated after 7 days of growth on potato dextrose agar (PDA, Condalab, Madrid, Spain) medium at 25°C. Microscopic parameters (conidium length, width and shape) were also measured under light microscopy at 40× magnification with the optical microscope

(Nikon Eclipse 80i, Nikon, Melville, NY, USA) in 0.05% Tween[®] 20 considering $n = 40$ conidia. All the isolates were maintained on PDA at 4°C and sub-cultured weekly.

Identification of *Trichoderma* Strains

Isolates were grown in potato dextrose broth (PDB, Condalab, Madrid, Spain) on a rotary shaker at 120 rpm for 96 h at 25°C. Fresh mycelium was collected after vacuum filtration through No. 4 Whatman filter paper (Whatman Biosystems Ltd., Maidstone, UK), then frozen in liquid nitrogen, ground to a fine powder and immediately processed. Total genomic DNA was extracted from 100 mg of ground mycelium by using the PureLink[®] Plant Total DNA Purification Kit (Invitrogen[™], ThermoFisher Scientific, Waltham, MA, USA) according to the manufacturer's protocol. PCR amplification of internal transcribed spacers and translation elongation factor 1 α (TEF1) was performed in a Biorad C1000 Thermal Cycler (Bio-Rad, Hercules, CA) following PCR program: denaturation at 96°C for 2 min; 35 cycles of denaturation at 94°C for 30 s; annealing at 55°C for 30 s; extension at 68°C for 75 s; final extension at 68°C for 10 min. Primers ITS1 (5'-CTTGGTCATTTAGAGGAAGTAA-3') and ITS4 (5'-TCCTCCGCTTATTGATATGC-3') were used to amplify a fragment (~0.6 kb) of rDNA including ITS1 and ITS2 and the 5.8S rDNA gene (White et al., 1990; Gardes and Bruns, 1993) while the 5' portions of translation elongation factor 1 α (~0.8 kb) coding region and introns were amplified with primers TEF1-F (5'-ATGGGTAAGGARGACAAGAC-3') and TEF1-R (5'-GGARGTACCAGTSATCATGTT-3'), which prime within conserved exons (O'Donnell et al., 1998). Amplicons were separated by gel electrophoresis in 1% w/v agarose supplemented with SYBR Safe DNA Gel Stain (Invitrogen, Paisley, UK). Amplicon sizes were determined against a 100 bp DNA ladder (Invitrogen[™], ThermoFisher Scientific, Waltham, MA, USA). PCR products were purified by PureLink[™] PCR Purification Kit (Invitrogen[™], ThermoFisher Scientific, Waltham, MA, USA) following the manufacturer's instructions, quantified with a NanoDrop[™] system (NanoDrop Technologies Inc., Wilmington, DE, USA) and sent to Sanger sequencing.

Phylogenetic Reconstruction

Phylogenetic relationships of the 16 *Trichoderma* strains were investigated based on ITS and TEF1 sequences. DNA sequences were blasted against the NCBI GenBank database using default parameters and then aligned with the more related *Trichoderma* isolates by the Clustal W algorithm (Thompson et al., 1994) with MEGA7 software (Kumar et al., 2016). Multiple alignments parameters were gap penalty = 10 and gap length penalty = 10. The default parameters (Ktuple = 2, gap penalty = 5, window = 4, and diagonals saved = 4) were used for the pairwise alignment. Final alignment adjustments were made manually in order to remove artificial gaps, as reported by Ospina-Giraldo et al. (1999). The analysis was conducted on the two gene partial sequences separately. Aligned sequences were then concatenated to a total length of 1,667 nucleotides. The evolutionary history was inferred using the maximum likelihood method. The evolutionary distances were computed

TABLE 1 | List of *Trichoderma* strains identified in this study with the GenBank accession numbers of the internal transcribed spacer (ITS) and translation elongation factor 1 α (TEF1) sequences.

Strains	ITS	TEF1	Species
Ta100	MW191738	MW201694	<i>Trichoderma atroviride</i>
Ta104	MW191739	MW201695	<i>Trichoderma atroviride</i>
Ta104C	MW191740	MW201689	<i>Trichoderma atroviride</i>
Ta104S	MW191741	MW201690	<i>Trichoderma atroviride</i>
Ta105	MW191742	MW201692	<i>Trichoderma atroviride</i>
Ta116	MW191743	MW201693	<i>Trichoderma atroviride</i>
Ta117	MW191744	MW201691	<i>Trichoderma atroviride</i>
Ti35	MW191751	MW201701	<i>Trichoderma longibrachiatum</i>
Ta56	MW191737	MW201688	<i>Trichoderma atroviride</i>
TaIC12	MW191745	MW246311	<i>Trichoderma atroviride</i>
Tat11	MW191747	MW201697	<i>Trichoderma atroviride</i>
Tat3C1	MW191746	MW201696	<i>Trichoderma atroviride</i>
ThCB	MW191749	MW201699	<i>Trichoderma harzianum</i>
ThRP	MW191750	MW201700	<i>Trichoderma harzianum</i>
Th23	MW191748	MW201698	<i>Trichoderma harzianum</i>
Ti41	MW191752	MW201702	<i>Trichoderma longibrachiatum</i>

using the Tamura-Nei model. The confidence of the branching was estimated by bootstrap (BP) analysis with 1,000 replications (1000 BP). *T. atroviride* sequences DAOM 233966, DAOM 231423, DAOM 233456, *T. longibrachiatum* sequences DAOM 231854, DAOM 232019 and DAOM 231850 and *T. harzianum* sequences DAOM 233458, DAOM 232032 and DAOM 232055, were used as references. All sequences were deposited in GenBank under the accession numbers reported in Table 1.

In vitro Dual Confrontation Assay

The ability of the sixteen *Trichoderma* strains to contain the development of *R. solani*, *S. sclerotiorum* and *S. rolfisii* *in vitro*, was evaluated by the dual culture technique. These phytopathogenic fungi were stored in the fungal collection of CREA-OF, maintained on PDA slants. Mycelial plugs of 5-mm diameter, obtained from the periphery of 7-days old cultures of both pathogen and *Trichoderma* strains were placed simultaneously on the border of the plate (9 cm diameter), about 0.25 mm from the edges at opposite sides. The Petri dishes containing PDA medium inoculated only with the pathogen were used as reference controls. All plates were incubated at 25°C and the radial growth was recorded 7-days post-inoculation. The growth inhibition percentage was calculated by using the formula:

$$\text{Growth inhibition (\%)} = 100 - \frac{C - T}{C}$$

where C = pathogen radial growth in the control and T = pathogen radial growth of the in the dual culture.

In vivo Biocontrol Activity Assays

The biocontrol activity of *Trichoderma* strains was assessed *in vivo* against *R. solani* on wild rocket, *S. sclerotiorum* on green baby lettuce and *S. rolfisii* on red baby lettuce.

One L flasks containing 150 g of common millet seeds were saturated with a $0.1 \times$ PDB (w/w) and autoclaved. Flasks were then inoculated with 15 plugs 5 mm diameter obtained from one-week-old plates of each pathogen maintained on PDA, and incubated for 21 days at 25°C. At the end of incubation, the inoculum was ground and added to sterilized peat soil at the final concentration of 1% (w/w) for *R. solani* and *S. rolfsii*, and 2% (w/w) for *S. sclerotiorum*, respectively, according to the pathogen virulence. In the uninfected pots, non-inoculated common millet prepared as described above, was added. *Trichoderma* spp. spore suspensions were obtained from one-week-old cultures maintained on PDA at 25°C. For each isolate, the conidia were harvested by washing the plates with sterilized water using a sterile brush. The suspension was filtered and collected in a 50 mL Falcon® tube (Falcon, USA). The spore suspension concentration was measured by a Burkler chamber (Brand, Germany) and adjusted at 1×10^7 spore mL⁻¹. Seeds of wild rocket cv. Tricia (Enza Zaden, Italy), green baby lettuce cv 166 (Sementi Dom Dotto, Italy) and red baby lettuce cv. Pamela (Maraldi, Italy) were sown in vermiculite-filled 500 mL bowls, germinated in the dark at 25°C and then maintained in a growth chamber at 22°C with a 12-h photoperiod. The irrigation was manually performed daily and a basal NPK mix liquid fertilization was applied twice a week. After 15 days, plants were transplanted in plastic pots (7 cm diameter and 100 mL volume capacity) filled with sterile peat, infected as described above. Each treatment consisted of three pots (replicates) containing 5 plants each for baby lettuces, and 10 plants *per* pot for rocket. After that, *Trichoderma* suspension treatments were applied by soil drenching reaching a final concentration of 1×10^6 spore mL⁻¹. Untreated infected pots and healthy pots were used as reference controls.

Pot distribution was arranged randomly in the growth chamber at the same conditions described above. After 7-days

incubation, each pot was assessed for hyperspectral images, disease incidence (DI%) and severity index (DSI). DI was calculated as the percentage of plants with disease symptoms on the total. Disease severity was assessed using a 1–3 scale adapted from Larkin and Honeycutt (2006): 0: no symptom; 1: foliar discoloration; 2: plant withering and visible lesion(s); 3: severe infection and plant dead.

DI% and DSI were calculated according to Yang et al. (2009). The experiment was performed twice.

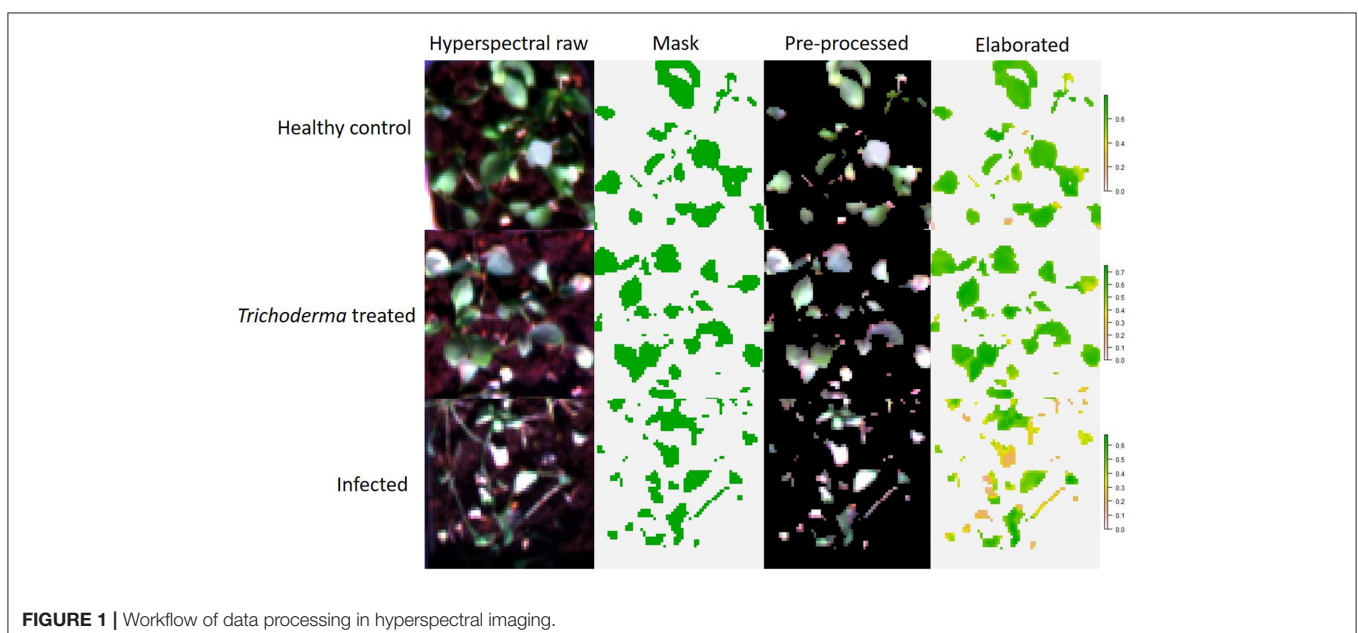
Hyperspectral Imaging

Hyperspectral images were acquired by using the SPECIM IQ camera (Specim, Spectral Imaging Ltd., Oulu, Finland) working in the range of 400–1,000 nm on a total of 204 wavelengths with a spectral resolution of 4 nm. The camera carries a CMOS sensor with a spatial sampling of 512 pixels and an image resolution of 512 × 512 pixel. The pixel size is 17.58 × 17.58 μm. Reflectance value was calculated automatically by the camera software. The images were captured under natural light conditions (Irradiance range 800–1,000 W/m²). One image *per* replicate (pot) was acquired, each containing all conditions (treatments) analyzed. Relative reflectance of hyperspectral images was simultaneously computed by the camera software. White reference, dark frame and raw data, were acquired during the measurements. The equation applied for the computation of the raw reflectance was as follows:

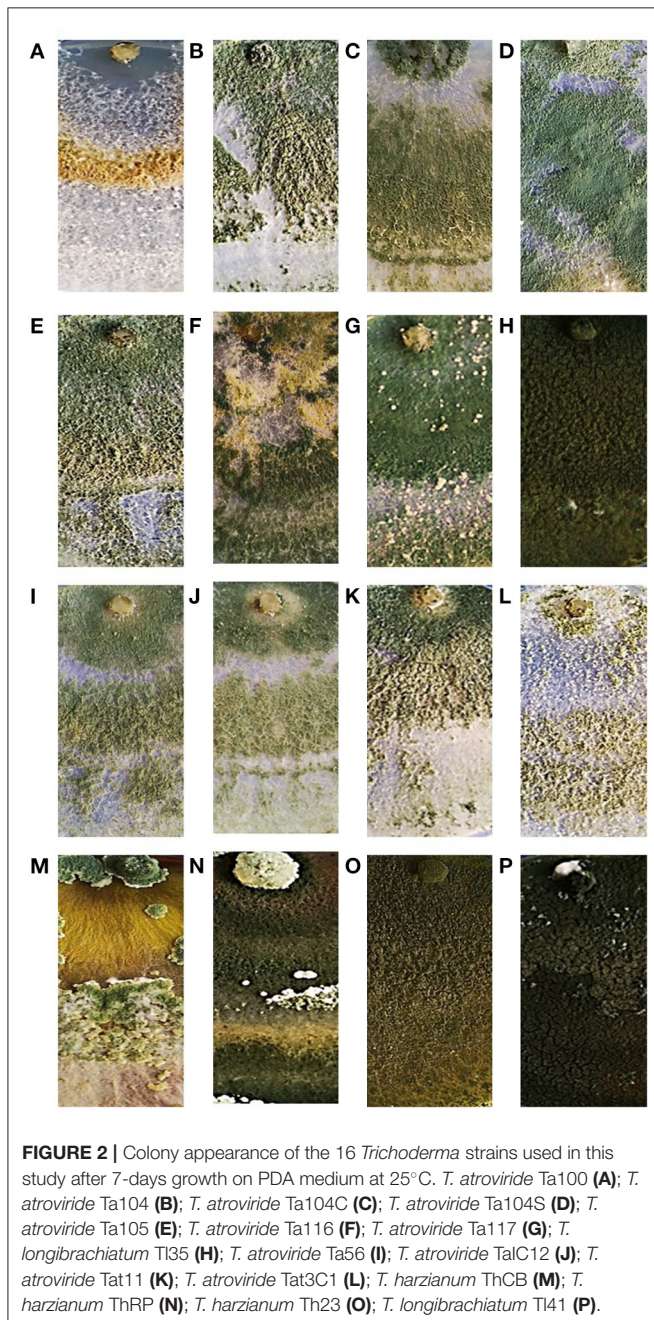
$$\text{Raw Reflectance} = \frac{(\text{Raw data})^{t1} - (\text{Dark})^{t1}}{(\text{White})^{t2} - (\text{Dark})^{t2}} \times \frac{t2}{t1}$$

where *White* is the white reference, *t1* and *t2* are integration times (used for a highly reflective white reference), and *Dark* represents a target with low reflectance.

The elaboration of the hyperspectral images was carried out with the R software. Raster R package (Hijmans et al., 2015) was



used to visualize and extract the hypercube dataset, successively elaborated into a typical spectral graphic. The unsupervised classification of the images was performed with Cluster R package to remove background once separated the objects “X” into “K” clusters. K-means clustering algorithm is a partitional or non-hierarchical clustering method (MacQueen, 1967; Anderberg, 1973), that here highlighted two clusters, background and plants (Figure 1). Then, the background cluster was deleted from the image, while the plant cluster was submitted to the extraction of the 46 hyperspectral VIs by imaging, averaging the pixel values for each replicate *per* treatment.



Hyperspectral Vegetation Indices and Statistical Analysis

Measurements of the pathogen growth inhibitions *in vitro*, disease incidence and disease severity percentages, were subjected to the statistical analysis by GraphPad Prism Software. Ordinary one-way ANOVA was applied to test the effects of the *Trichoderma* strains on the assessed parameters. In all cases, the statistical analysis of variance was corrected for multiple comparisons by the Bonferroni hypothesis test, considering a p -value ≤ 0.05 . Since experiment effect was not observed, data from the repeated experiments were pooled.

The same procedure was applied to evaluate the indices calculated on the hyperspectral dataset. Moreover, in order to select the most informative ones, they were analyzed, in relation to the observed disease severity in each pathosystem, by Multiple Variable analysis, applying the Pearson's correlation coefficient. The high-performing VIs that resulted commons to all the three host-pathogen target systems, were filtered on the base of a stringent statistical grid (p -value ≤ 0.05 and $R^2 > 0.5$) and highlighted by using Venn diagram (<http://bioinformatics.psb.ugent.be/webtools/Venn/>). The heatmap visualization and the hierarchical clustering analysis of the selected indices were obtained applying ClustVis online software (<https://bit.cs.ut.ee/clustvis>). Unit variance scaling was applied to rows and columns and they were clustered using correlation distance and average linkage. Furthermore, the Principal Component Analysis (PCA) of vegetative indices / disease index for each pathosystem was performed with the *pca* function of the R Factoextra package (Kassambara and Mundt, 2017). Data were log-normalized and disease severity index was converted to “factor” by grouping in classes according to the following 0–4 scale: 0 = $0 \leq \text{DSI} \leq 0.2$; 1 = $0.21 \leq \text{DSI} \leq 0.4$; 2 = $0.41 \leq \text{DSI} \leq 0.6$; 3 = $0.61 \leq \text{DSI} \leq 0.8$, 4 = $0.81 \leq \text{DSI} \leq 1$. Then, *lm* function (R package) was applied to fit linear models.

RESULTS

Colony and Conidium Morphological Characteristics

The morphological characterization of the sixteen *Trichoderma* isolates studied in this work was carried out based on the inoculated medium appearance and pigmentation, color and edge of colonies, culture smell, shape and size of the conidia. After 5-days incubation at 25°C, the growth and sporulation patterns of the *Trichoderma* isolates showed significant differences. During the growth, due to the release of secondary metabolites, medium pigmentation varied significantly among the *Trichoderma* isolates, ranging from colorless to bright yellow and yellow-brownish to amber. Some of them showed a profuse production of conidia with coloration ranging from white to dark green (Figure 2). Furthermore, microscopic observations allowed highlighting differences in terms of conidia size and shape. In fact, the conidia of Ta56, Ta117, Ta105, ThRP, and Tat3C1

TABLE 2 | Main morphological features of colonies (medium pigmentation, color, edge and smell) and conidia (length, width, length-to-width ratio and shape) of the *Trichoderma* strains used in this study.

Strains	Colonies				Conidia			
	Medium pigmentation	Color	Edge	Smell	Length (μm)	Width (μm)	L/W ratio	Shape
Ta100	Uncolored	White	Smooth	-	4.5 \pm 0.3	4.09 \pm 0.2	1.13 \pm 0.20	Ellipsoidal
Ta104	Uncolored	Dull green to bluish green	Smooth	-	3.9 \pm 0.2	3.3 \pm 0.3	1.22 \pm 0.31	Ellipsoidal
Ta104C	Uncolored	Dull green to bluish green	Smooth	-	4.5 \pm 0.3	4.1 \pm 0.3	1.16 \pm 0.22	Ellipsoidal
Ta104S	Uncolored	Dark green	Smooth	-	4.3 \pm 0.3	3.77 \pm 0.4	1.17 \pm 0.16	Ellipsoidal
Ta105	Uncolored	Dull green to bluish green	Smooth	-	3.8 \pm 0.3	3.8 \pm 0.3	1.02 \pm 0.21	Sphaeric
Ta116	Uncolored	Yellow to dark green	Smooth	-	4.5 \pm 0.3	3.6 \pm 0.4	1.27 \pm 0.24	Ellipsoidal
Ta117	Uncolored	Dark green	Smooth	-	4.3 \pm 0.2	4.2 \pm 0.3	1.04 \pm 0.21	Sphaeric
TI 35	Yellow-greenish	Dark green-white tufts	Smooth	-	4.7 \pm 0.5	3 \pm 0.1	1.39 \pm 0.28	Ellipsoidal
Ta56	Uncolored	Dull green to bluish green	Smooth	coconut	4.0 \pm 0.4	4.1 \pm 0.3	1.00 \pm 1.15	Sphaeric
TaIC12	Uncolored	Dull green to bluish green	Smooth	coconut	4.6 \pm 0.4	4.1 \pm 0.3	1.17 \pm 0.27	Ellipsoidal
Tat11	Uncolored	Dull green to bluish green	Smooth	coconut	5.4 \pm 0.3	4.8 \pm 0.2	1.14 \pm 0.24	Ellipsoidal
Tat3C1	Uncolored	White-green	Wavy	-	4.2 \pm 0.1	4 \pm 0.2	1.09 \pm 0.21	Sphaeric
ThCB	Amber	Scattered in tufts, yellow green	Wavy	-	3.7 \pm 0.2	3.3 \pm 0.2	1.14 \pm 0.24	Ellipsoidal
ThRP	Yellow-brownish	Dark green	Smooth	-	4.9 \pm 0.5	4.8 \pm 0.5	1.05 \pm 0.26	Sphaeric
Th 23	Bright yellow	Dark green-white tufts	Smooth	-	4.1 \pm 0.2	3 \pm 0.4	1.41 \pm 0.25	Ellipsoidal
TI41	Yellow-orange	Dark green	Smooth	-	4 \pm 0.4	3.5 \pm 0.3	1.20 \pm 0.32	Ellipsoidal

isolates, showed spherical shape with length-to-width ratio around 1, while the conidia of all the remaining strains, resulted ellipsoidal with length-to-width ratio > 1 . The morphological colony and conidium features are summarized in **Table 2**.

Determination of *Trichoderma* Species

The multi-locus sequence analysis is suggested for a better distribution of *Trichoderma* spp. in a phylogenetic tree (Samuels et al., 2010). Therefore, in the present work, concatemers of the ITS-TEF1 genes were used to construct the phylogenetic tree inferred by neighbor-joining method, as reported by Ospina-Giraldo et al. (1999). rDNA region and partial translated elongation factor locus amplifications, yielded products of ~ 600 and 800 bp, respectively, as estimated by agarose gel electrophoresis. Loci were analyzed separately, aligned and manually adjusted. Sequences were then grouped in concatemers and subjected to the phylogenetic analysis. This analysis involved 26 nucleotide sequences with a total of 1,667 positions in the final dataset. Based on the bootstrap values, the 16 *Trichoderma* strains were arranged into three distinct groups, belonging to *T. atroviride*, *T. longibrachiatum* and *T. harzianum* species (**Figure 3**). The strains Ta100, Ta104, Ta104C, Ta104S, Ta105, Ta116, Ta117, Ta56, Tat11, TaIC12, and Tat3C1, clustered within the *T. atroviride* clade, resulting aligned with the reference strains (DAOM 233966, DAOM 231423, and DAOM 233456). On the other hand, TI35 and TI41 strains were identified as *T. longibrachiatum*, showing a strictly association with the reference isolates (DAOM 231854, DAOM 232019, and DAOM 231850), while the strains Th23, ThRP and ThCB clustered in the *T. harzianum* clade. These identifications resulted well-supported by bootstrap tests, with values $> 60\%$.

In vitro Dual Challenge Assay

The dual culture assay was optimized to compare the inhibition activity of the 16 *Trichoderma* strains against the three soil-borne fungal pathogens. Since no significant differences were observed in the timing of growth among *Trichoderma* strains, *S. sclerotiorum*, *R. solani*, and *S. rolfsii*, the fungi were co-inoculated. As reported in **Figure 4**, all *Trichoderma* strains determined around 60% inhibition of *S. sclerotiorum* and *R. solani* radial growth. Only slight differences were observed among the different *Trichoderma* strains in inhibiting those phytopathogenic fungi. Furthermore, all the biocontrol strains, except Ta100 and Th23, reached the pathogen in 4–5 days and overgrew it in 9–10 days. On the other hand, most of the *Trichoderma* strains showed the ability to inhibit *S. rolfsii* radial growth up to 70%. Additionally, significant differences were observed among the different *Trichoderma* strains in containing this pathogen. In fact, a profuse overgrowth was observed for Ta116, ThRP, Ta105, Tat11, ThCB, Ta104C, Ta56, TaIC12, and Ta104S after 9 days, while TI35 and Th23 resulted less effective in reducing the *in vitro* fungus development.

In vivo Biocontrol Activity

The ability of the different *Trichoderma* strains to protect plants was investigated by *in vivo* assays with *R. solani* on wild rocket, *S. sclerotiorum* on green baby lettuce and *S. rolfsii* on red baby lettuce. On all cases, disease incidence percentages (**Figure 5** left) and disease severity index (**Figure 5** right) were assessed. Overall, a significant *Trichoderma* treatment effect was found (p -value < 0.001), as well as the interaction between factor *Trichoderma* strain \times plant/pathogen system (p -value < 0.001). The application of Ta116, TI35, Ta56, TaIC12, Tat3C1, and TI41, on wild rocket significantly reduced the percentage of Rhizoctonia disease incidence detected 120 h post-inoculation, in

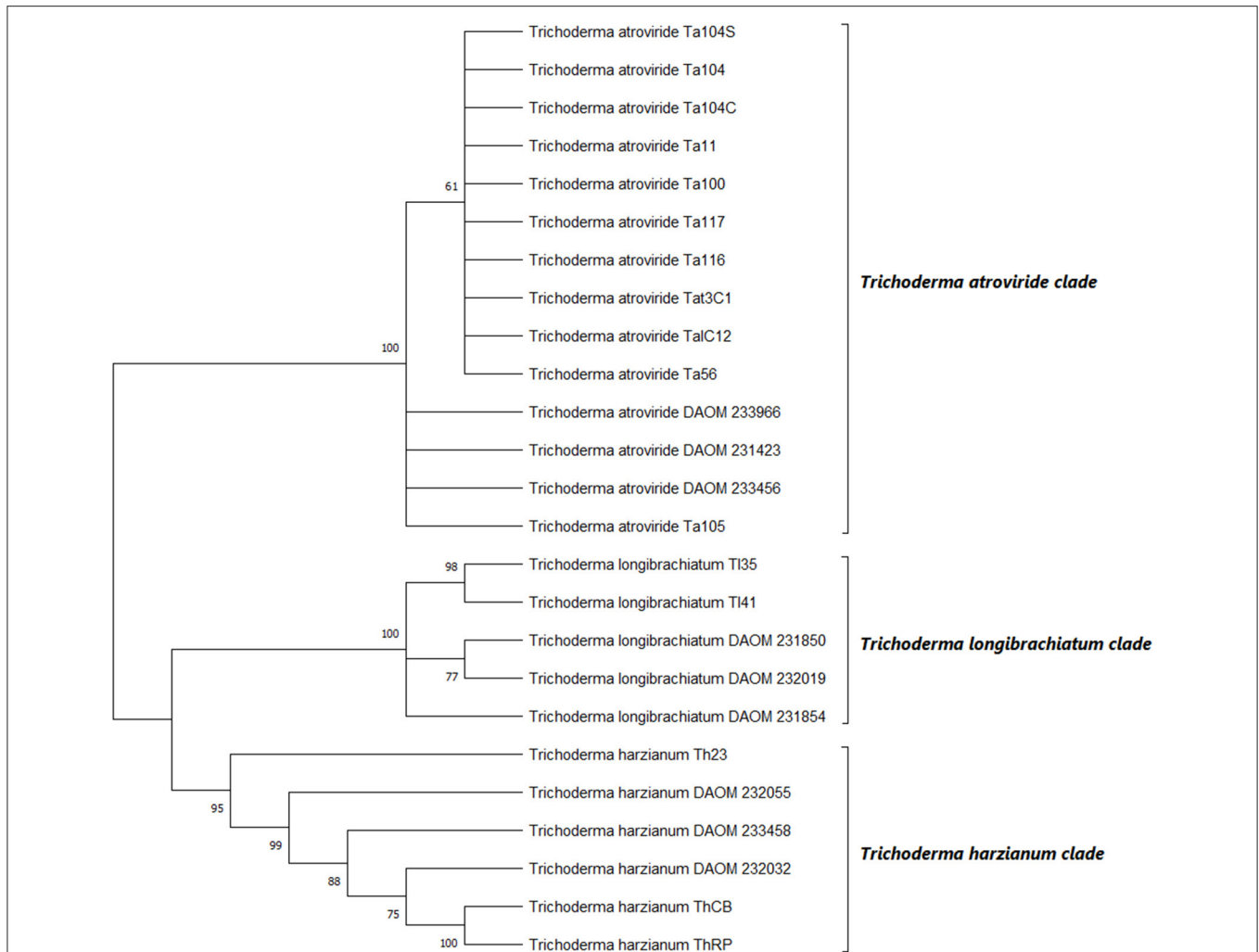


FIGURE 3 | Phylogenetic relationships among the 16 strains of *Trichoderma* spp. inferred by analysis of rDNA (ITS) and translation elongation factor 1- α (TEF1) concatemers. The evolutionary history was inferred using the maximum likelihood method. The optimal tree is shown. The percentage of replicate trees in which the associated taxa clustered together in the bootstrap test (1000 replicates) are shown next to the branches. The evolutionary distances were computed by applying Tamura-Nei model. DAOM 233966, DAOM 231423 and DAOM 233456 (*T. atroviride*); DAOM 231854, DAOM 232019 and DAOM 231850 (*T. longibrachiatum*); DAOM 233458, DAOM 232032 and DAOM 232055 (*T. harzianum*) are the reference sequences.

comparison with the infected control. In fact, only the 60% of TI35 treated plants showed disease symptoms; for all the other treatments, the disease incidence was around 80%. Interestingly, all *Trichoderma* strains, except for Tat11 and Th23, contained the severity of the disease: the bio-treated plants displayed mild disease symptoms or were almost healthy.

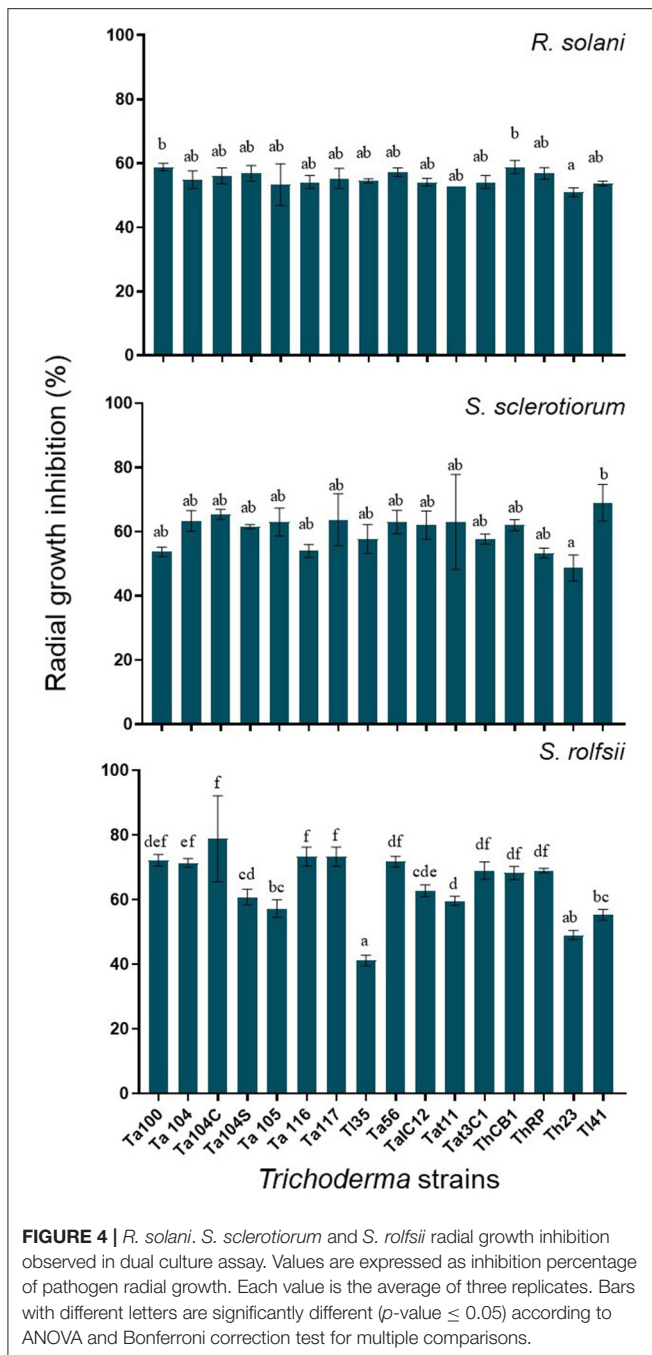
On the other hand, the BCAs reduced *Sclerotinia* disease incidence on green baby lettuce, excepted for Ta104, Ta104S and ThRP; the number of plants with symptoms was significantly lower than that observed in the infected control and a consistent reduction in the disease severity index was also observed.

Trichoderma harzianum Th23 resulted the best one in containing *Sclerotinia* disease development. The strains Ta100, Ta104, Ta117, TI35, Ta56, Tat11, ThCB, ThRP, and Th23, were able to control *S. rolfsii* on red baby lettuce determining a

meaningful reduction of disease incidence. Furthermore, all *Trichoderma* treated plants, excepted for Ta104S, TaIC12, and Tat11 interactions, showed a significant lower disease severity index than the infected control.

Hyperspectral Imaging

Plants infected with the three soil-borne pathogens and exposed to the biocontrol treatment with *Trichoderma*, were subjected to hyperspectral imaging analysis in order to capture the spectral changes that occurred during the plant-pathogen-antagonist relation. As reported in **Figure 5A**, out of the 46 analyzed hyperspectral indices, 13 significantly cross-correlated with *Rhizoctonia* disease on rocket, 26 with *Sclerotinia* drop on green baby lettuce and 7 with *Sclerotium* rotting on red baby lettuce. Interestingly, four indices, OSAVI, SAVI, TSAVI



and TVI, resulted shared by the three assayed pathosystems. The Multiple Variable analysis showed the score of their negative cross-correlation with the disease severity index for each plant/pathogen systems, with samples distributing between the two extremes, full healthy and full diseased (Figure 6B), coherently with changes visualized in the spectral signatures among non-inoculated, infected and infected but bio-treated plants (Figure 7A). Hence, heatmap visualization of the VIs/DSI hierarchical clustering quickly identified the most effective

biocontrol agents in relation to the specific pathosystem (Figure 7B).

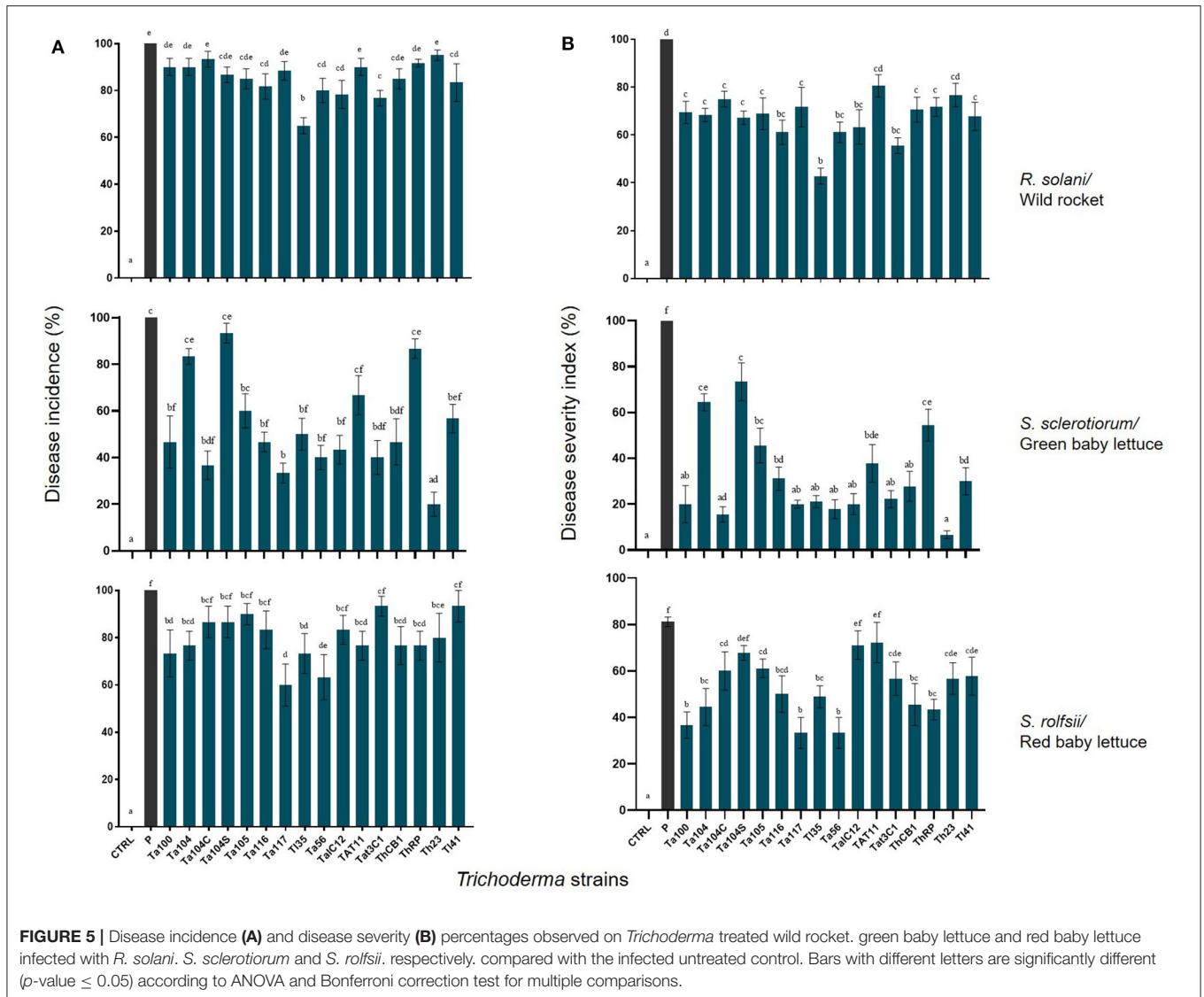
PCA analysis of VIs detected in the three different pathosystems showed their consistent ability to discriminate among different disease levels (Figure 8). Furthermore, OSAVI, SAVI and TSAVI resulted quite redundant, probably due to they differ only in the algorithm used for combining spectral data, while the distinct contribution in explaining the variance along PC1 (93.9%) was associated to TVI (Figure 8).

In order to fit a linear model, DSI data and selected indices were analyzed for multiple regression (Table 3). Based on the PCA results, SAVI indices (OSAVI, SAVI and TSAVI) computed together and TVI were submitted to linear regression analysis. OSAVI index was excluded since OSAVI:TVI interaction was found not significant in the resulting linear model. Results showed that F-statistic was highly significant ($< 3.5e-10$) meaning that at least, one of the predictor is significantly related to the outcome variable. All the coefficients, including the interaction term coefficients, were statistically significant, suggesting that there is an interaction between the two predictor variables TSAVI + SAVI and TVI. On the other hand, these last are able to provide information about the biological observations although R-squared value was low. Thereby, statistical outputs corroborated the visualization by VIs images of the effects of *Trichoderma* strains on the disease symptom expressions over the cultivars.

Differences between healthy and diseased controls resulted, actually, perceptible on OSAVI, SAVI, TSAVI and TVI images, and the BCA treated plants displayed intermediate collocations (Figures 9–11). However, the correlational analysis identified disease-specific indices as reported in Figure 6A. Indeed, MCARI and SRPI resulted effective to track the *R. solani*/wild rocket interaction, other 15 indices (ARI, CAR, LRDSI, msr705, NDVI, PRI, PSSRc, R705, RDVI, RGRcn, RVI, RSVI, SIPI, TCARI, VARI-Green) were found significantly correlated to the *S. sclerotiorum* infection degree of green baby lettuce, while LIC3, VOG2, VOG3 were found suitable for following the *S. rolfsii*/red baby lettuce interaction. A summarization of Pearson's analysis involving all the VIs, is reported in Table 4.

DISCUSSION

Trichoderma spp. include a plethora of isolates with biocontrol activity against phytopathogens (Kumar et al., 2017) that can also give additional benefits to the plants, such as increase the nutrient uptake, enhance the photosynthetic activity and stimulate different metabolic processes that positively affect yields and quality of the treated crops (El Enshasy et al., 2020). Recently, it has been shown that soil treatment with *Trichoderma* gave biostimulant effects on wild rocket and baby lettuce, ranging from the increase of leaf yield, fresh and dry weight, to the improvement of leaf nutritional status, resulting in a premium quality of the fresh-cuttings with higher lipophilic antioxidant activity and total ascorbic acid content (Fiorentino et al., 2018; Caruso et al., 2020; Di Mola et al., 2020; Rouphael et al., 2020). However, expressing the full biocontrol potential



in these contexts, *Trichoderma*-based formulates can successfully integrate disease management protocols for producing baby leaf vegetables with high added value in terms of sustainability, decreasing the dependence on synthetic fungicides.

This study recruited sixteen new *Trichoderma* antagonistic strains assigned, on the base of the variations of the rRNA ITS and translation elongation factor 1- α gene partial sequences, to three different species, *T. longibrachiatum*, *T. atroviride*, and *T. harzianum*. Several stains of these species are well-known as BCAs of many pathogens affecting vegetables, including our targets (Bastakoti et al., 2017): they are proposed alone, being part of complex microbial consortia or activating suppressive organic amendments (Kareem et al., 2016; Wang et al., 2019; Chilosi et al., 2020). The macroscopic and microscopic examination of the selected strains showed interesting characters such as the profuse sporulation, the ability to secrete secondary metabolites in the medium changing its pigmentation and the capability of some to produce a volatile compound with the typical coconut-like

aroma. This last specific character was detected in the strains Ta56, Ta1C2, and Tat11 and could be putatively associated to the production of 6-pentyl- α -pyrone, a bioactive unsaturated δ -lactone with interesting properties involved in the microbial antagonism (Bonnarme et al., 1997; Serrano-Carreón et al., 2004; Longo and Sanromán, 2006; Ramos et al., 2008; Penha et al., 2012; Pascale et al., 2017). However, to clarify these aspects, further metabolomic investigations are necessary.

All the new identified antagonists significantly inhibited the mycelial growth of the pathogens in the dual culture assay. The main mechanism of control resulted to be the mycoparasitism, highlighted by the overgrowth of the BCAs onto the pathogen mycelia, observed already after 9–10 days of incubation. Mycoparasitism is one of the major weapons displayed by *Trichoderma* spp. against phytopathogens (Sachdev and Singh, 2020) allowing them to parasitize and kill the fungal host after the direct contact. During this intimate interaction, the beneficial fungus produces antibiotics and a

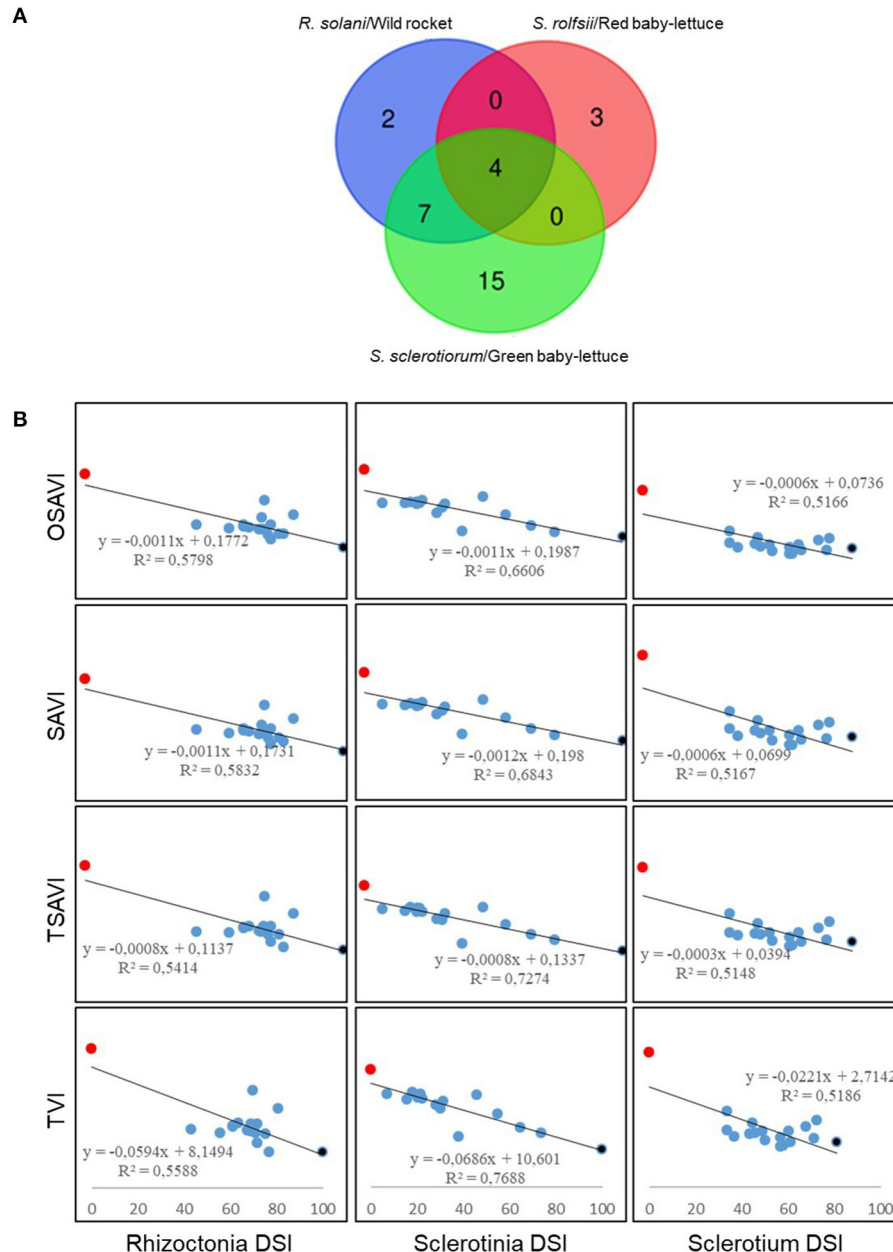


FIGURE 6 | Selection of the significant (p -value ≤ 0.05 and $R^2 > 0.5$) cross-correlated hyperspectral vegetation indices with disease severity index (DSI) for *R. solani*/wild rocket, *S. sclerotiorum*/green baby-lettuce and *S. rolfsii*/red baby-lettuce compatible interactions. **(A)** Venn diagram showing the number of the vegetative indices significantly cross-correlated with disease severity, common and not common to all the pathosystems. **(B)** Pearson's correlation between the common hyperspectral vegetative indices (OSAVI, SAVI, TSAVI and TVI) and DSIs. Non-inoculated healthy controls (red); infected plants (black); infected plants treated with *Trichoderma* strains (blue).

huge array of cell degrading enzyme (protease, as β -glucanase, chitinase) necessary for the parasitism process (Steyaert et al., 2003).

In vivo biocontrol assays classified the *Trichoderma* BCA-candidates for the substantial ability to protect wild rocket, red and green baby lettuces from their most feared telluric fungal pathogens. Contrary to what was observed in *in vitro* assays,

the *in planta* trials showed meaningful differences in biocontrol intensity among the strains in relation to the target pathosystem.

Specifically, Tl35, Ta56, Ta116, TaIC12, and Tat3C1 resulted the most effective strains in controlling *Rhizoctonia* damping-off of wild rocket, determining a significant reduction in terms of DSI (roughly 60%) compared with infected control under high disease pressure (100%). *Rhizoctonia* crown and root rot

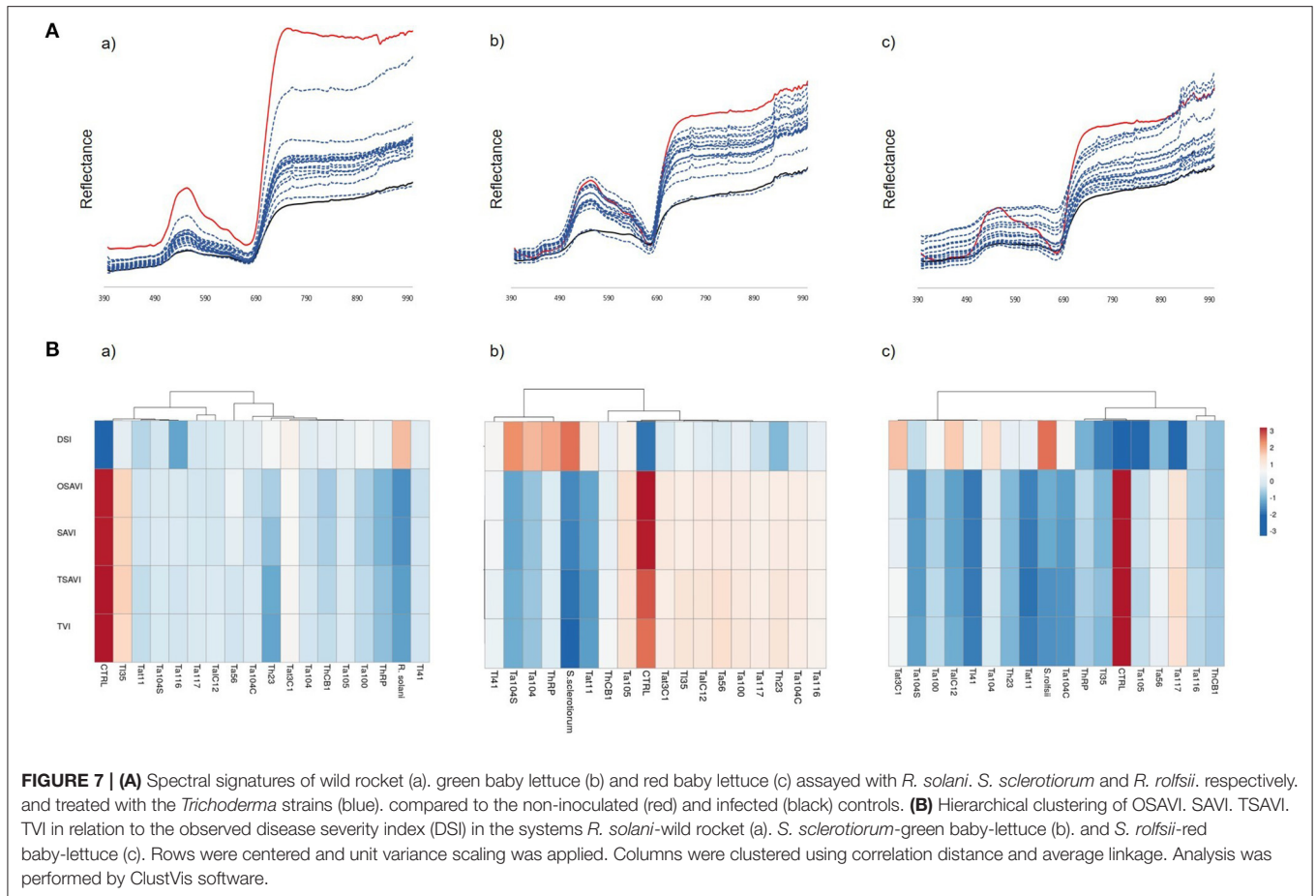


FIGURE 7 | (A) Spectral signatures of wild rocket (a), green baby lettuce (b) and red baby lettuce (c) assayed with *R. solani*, *S. sclerotiorum* and *R. rolfsii*, respectively, and treated with the *Trichoderma* strains (blue), compared to the non-inoculated (red) and infected (black) controls. **(B)** Hierarchical clustering of OSAVI, SAVI, TSAVI, TVI in relation to the observed disease severity index (DSI) in the systems *R. solani*-wild rocket (a), *S. sclerotiorum*-green baby-lettuce (b), and *S. rolfsii*-red baby-lettuce (c). Rows were centered and unit variance scaling was applied. Columns were clustered using correlation distance and average linkage. Analysis was performed by ClustVis software.

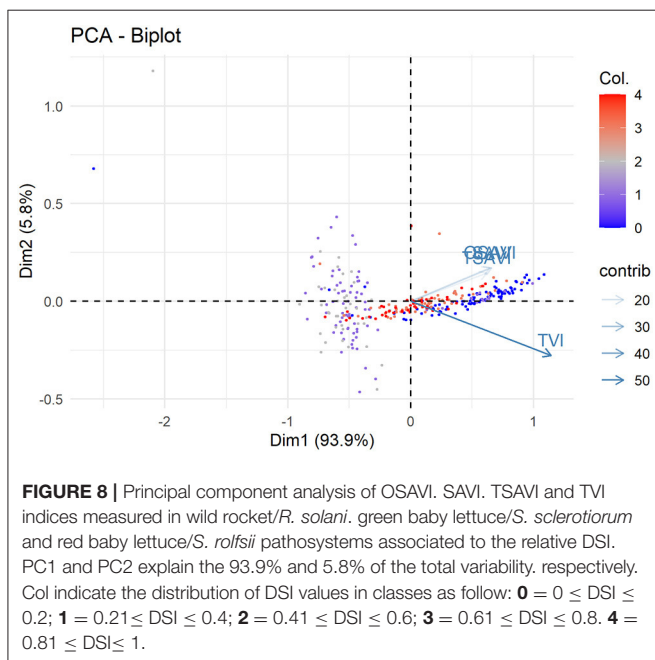


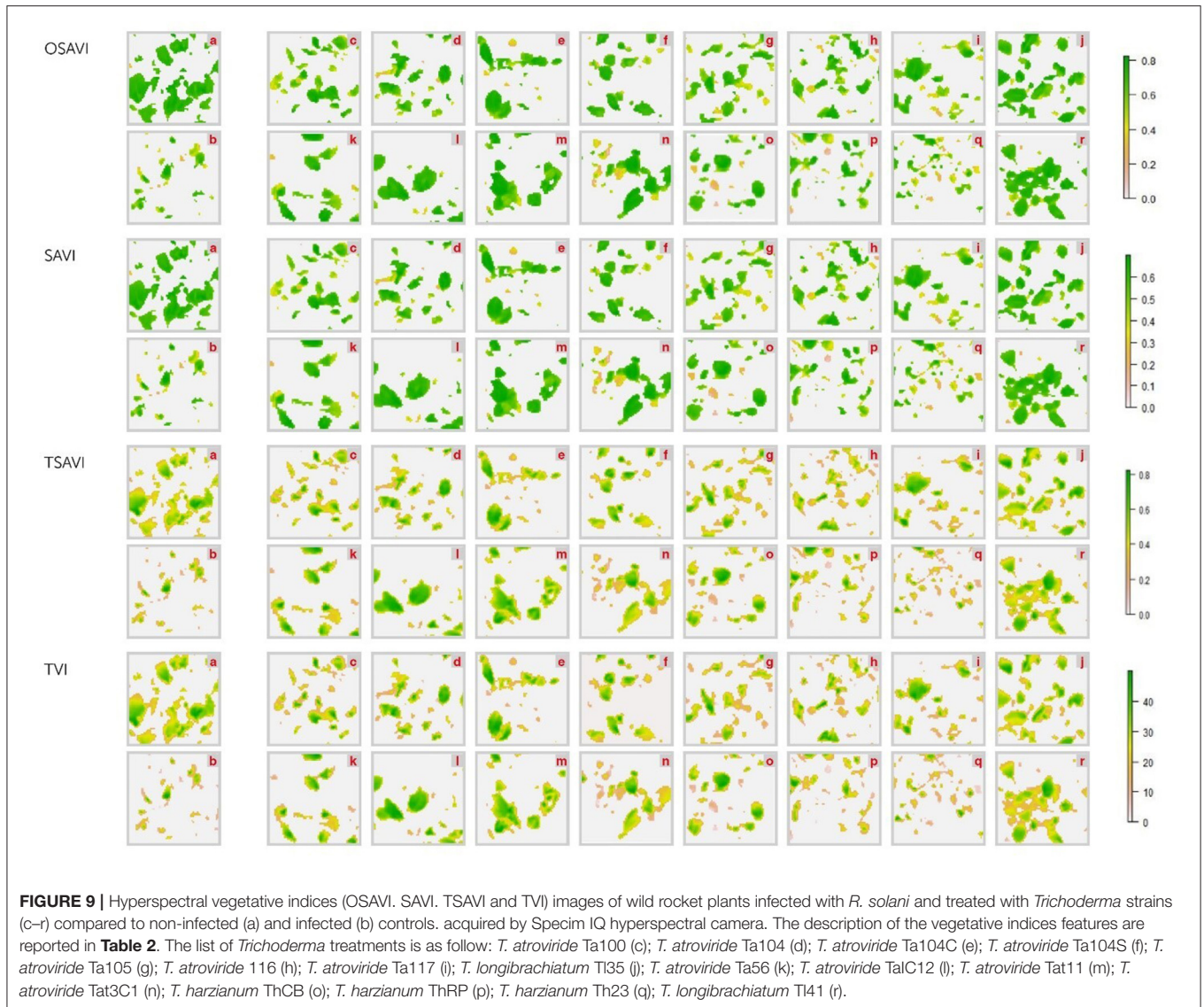
FIGURE 8 | Principal component analysis of OSAVI, SAVI, TSAVI and TVI indices measured in wild rocket/*R. solani*, green baby lettuce/*S. sclerotiorum* and red baby lettuce/*S. rolfsii* pathosystems associated to the relative DSI. PC1 and PC2 explain the 93.9% and 5.8% of the total variability, respectively. Col indicate the distribution of DSI values in classes as follow: **0** = $0 \leq DSI \leq 0.2$; **1** = $0.21 \leq DSI \leq 0.4$; **2** = $0.41 \leq DSI \leq 0.6$; **3** = $0.61 \leq DSI \leq 0.8$. **4** = $0.81 \leq DSI \leq 1$.

TABLE 3 | Summary of statistical values associated to linear regression model for prediction of DSI using SAVI (OSAVI, SAVI and TSAVI) and TVI vegetative indices.

Residuals					
	Min	1Q	Median	3Q	Max
	-0.53359	-0.24166	-0.02817	0.22259	0.63078
Coefficients					
	Estimate	Std. Error	tvalue	Pr(> t)	Signif.
(Intercept)	0.23261	0.05218	4.458	1.15E-05	***
TSAVI	-14.1965	4.65149	-3.052	0.002465	**
SAVI	10.91309	2.58815	4.217	3.24E-05	***
TVI	0.06265	0.02652	2.362	0.018777	*
TSAVI:	1.56296	0.61288	2.55	0.011235	*
TVI					
SAVI:	-1.45497	0.4281	-3.399	0.000763	***
TVI					

Residual standard error: 0.2812 on 318 degrees of freedom.
 Multiple R-squared: 0.1526. Adjusted R-squared: 0.1393.
 F-statistic: 11.46 on 5 and 318 DF. p-value: 3.5e-10.

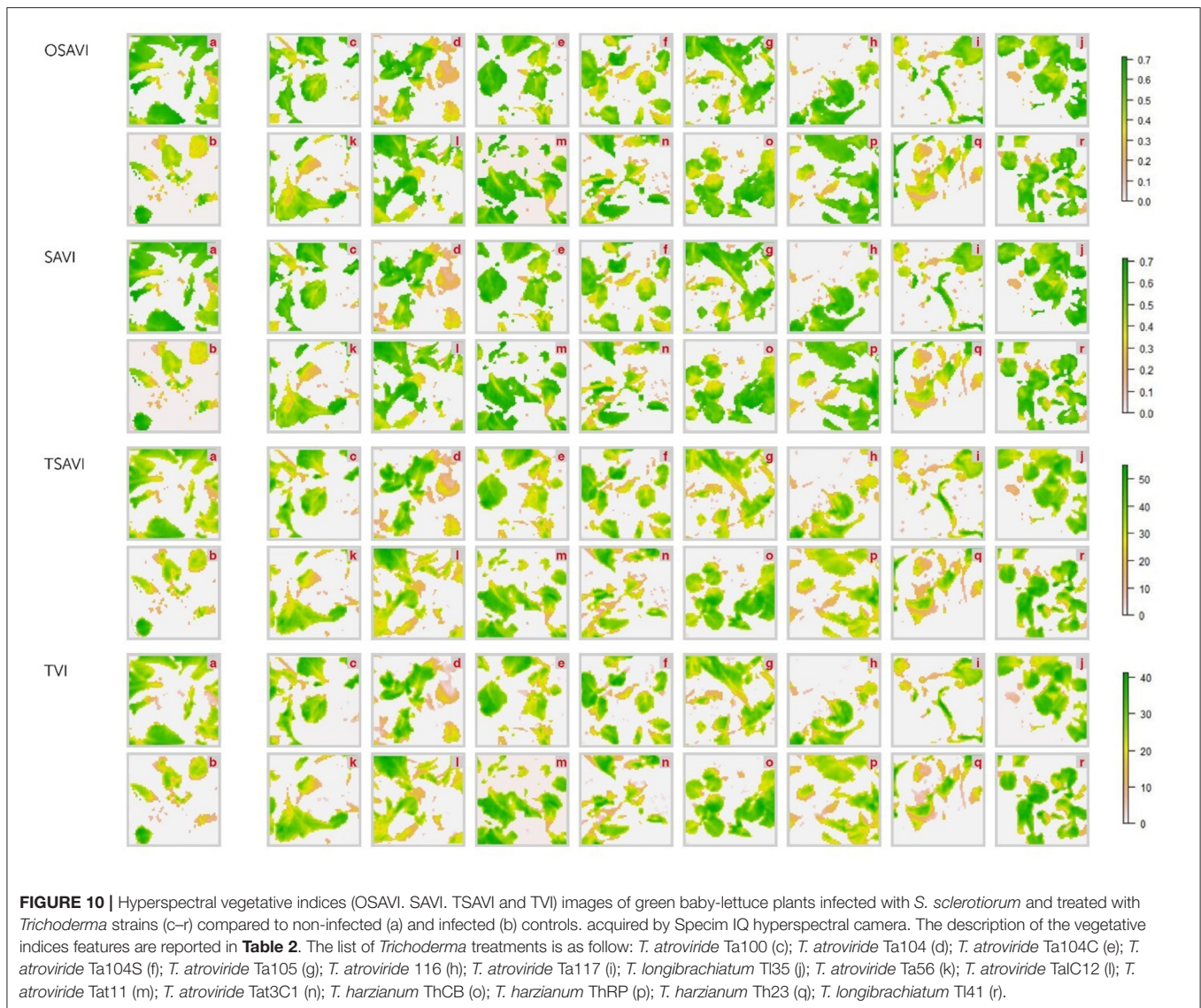
* $P \leq 0.05$; ** $P \leq 0.01$; *** $P \leq 0.001$.



is a problematic disease of wild rocket for the ready-to-eat produces in the Italian cropping areas (Nicoletti et al., 2004). For their biological control, only the hyperparasite *Clonostachys rosea* has been noticed in literature (Nicoletti et al., 2007). Genetic resistance to this pathogen is not available yet (Pane et al., 2017), while wild rocket waste meals are proposed as amendments to promote the soil general suppressiveness providing antifungal molecules contained into the grounded plant tissues (Schlatter et al., 2017). Our results suggest that *Trichoderma* spp. can reduce the incidence and the severity of the disease and earn a chance as effective antagonist in Rhizoctonia damping-off management.

On the other hand, the biological control of *Sclerotinia* species, in particular *S. sclerotiorum*, has received increasing attention on adult lettuce inasmuch as chemical control of this pathogen is usually difficult, because the ascospores can infect any part of the head and sclerotia resist in the soil and can occur after prolonged wet periods (Patterson and Grogan,

1985; Elias et al., 2016; Subbarao et al., 2017). Therefore, the antagonists play a crucial role in the lettuce drop management because of their ability to parasitize the sclerotia in deep soil layers (Subbarao, 1998). As *Sclerotinia* drop biocontrol agents, *Coniothyrium minitans* Campbell, *Clonostachys rosea* (Schroers et al., 1999) and *Trichoderma* spp. resulted effective either in laboratory or in soil assays (Turner and Tribe, 1976; Phillips, 1989; Whipps and Budge, 1990; Jones et al., 2003; Bonini et al., 2020). Furthermore, against the compatible interaction between *Sclerotinia* spp. and adult lettuces, *Trichoderma* biocontrol agents have been reported to effectively reduce the seedlings drop (Elias et al., 2016), promote plant growth under infection (da Silva et al., 2019) and delay the symptoms appearance by emitting volatiles (da Silva et al., 2021). Accordingly, our results on baby lettuces demonstrated that *Trichoderma* strains Ta100, Ta104C, Ta117, Tl35, Ta56, TaIC12, Tat3C1, ThCB, and Th23, belonging to different species, can contain *Sclerotinia* drop disease, reaching a



significant reduction of DSI (around 30%) compared to untreated control (DSI 100%).

Many previous studies reported the effectiveness of *Trichoderma* volatile compounds in inhibiting *S. rolfisii* growth (Hirpara et al., 2017; Marques et al., 2018; Sridharan et al., 2020). The culture filtrates with the highest antifungal effect against *S. rolfisii* were those of *T. brevicompactum* (Marques et al., 2018), *T. harzianum* (Saxena et al., 2014), *T. viride* (Darvin, 2013) and *T. virens* (Srinivasa and Devi, 2014). Wonglom et al. (2019) selected a *Trichoderma* strain with higher biocontrol properties against *Sclerotium* stem rot on red oak lettuce, due to its capability to produce volatile antifungal compounds (phenylethyl alcohol and epi-cubenol) and the cell wall degrading enzyme β -1,3-glucanase. Similarly, our results showed that *Trichoderma* strains Ta100, Ta104, Ta116, Ta117, Tl35, Ta56, ThCB1, and ThRP, highly suppressed lettuce *Sclerotium* rotting with a reduction of DSI around 50%, on average, compared to untreated infected control.

Interestingly, *T. atroviride* strain TA56 and *T. longibrachiatum* strain TA35 resulted to be multi-suppressive, namely highly effective in containing all the three diseases of the baby-leaf vegetables, demonstrating positive performances both *in vitro* and *in vivo*. The ability of these two BCAs to control the main disease of baby leaf make them promising candidates for a wide-spectrum application in preventive and/curative biological control practices in fresh-cut salad cropping, especially under soil sickness conditions.

Hyperspectral imaging was used here to objectively assess the biocontrol effectiveness of the comparing *Trichoderma* spp., interpreting the canopy reflectance response to the bio-treatments acquired by a hyperspectral sensor and summarized by VIs, thus, quantifying the functional effects. Four out of the 46 tried VIs, previously calibrated on plant physiological and structural shifts (Mishra et al., 2017), displayed significant (p -value < 0.05, highest coefficient of determination R^2) positive

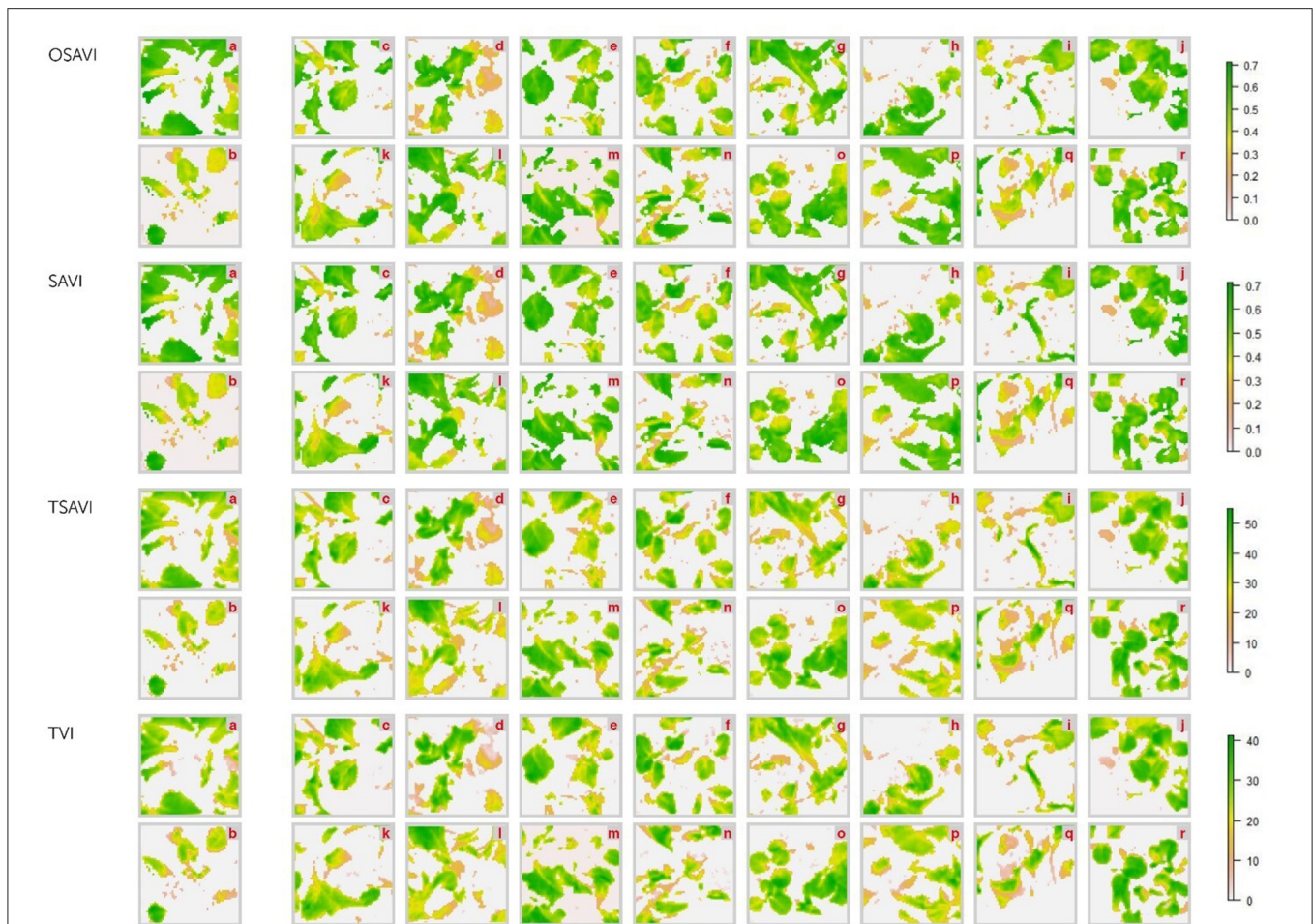


FIGURE 11 | Hyperspectral vegetative indices (OSAVI, SAVI, TSAVI and TVI) images of red baby lettuce plants infected with *S. rolfsii* and treated with *Trichoderma* strains (c–r) compared to non-infected (a) and infected (b) controls, acquired by Specim IQ hyperspectral camera. The description of the vegetative indices features are reported in **Table 2**. The list of *Trichoderma* treatments is as follow: *T. atroviride* Ta100 (c); *T. atroviride* Ta104 (d); *T. atroviride* Ta104C (e); *T. atroviride* Ta104S (f); *T. atroviride* Ta105 (g); *T. atroviride* 116 (h); *T. atroviride* Ta117 (i); *T. longibrachiatum* Tl35 (j); *T. atroviride* Ta56 (k); *T. atroviride* Ta1C12 (l); *T. atroviride* Tat11 (m); *T. atroviride* Tat3C1 (n); *T. harzianum* ThCb (o); *T. harzianum* ThRP (p); *T. harzianum* Th23 (q); *T. longibrachiatum* Tl41 (r).

relationships with plant health, as variably modulated by the biological control treatments contemporary in all the three target systems. The indices OSAVI, SAVI, TSAVI and TVI were able to highlight the most effective BCAs in controlling multiple soil-borne diseases of baby leaf vegetables. This result confirmed that selected indices can be applied as highly-informative tool for both BCA selections and disease monitoring in the presence of soil-borne pathogens generally associated to root and collar rot and, in advancing, leaf withering and plant death.

Therefore, the disease progression significantly affects the vegetation vitality and also the chlorophyll content. OSAVI, SAVI and TSAVI are soil adjusted vegetation indices, also defined as soil-line indices descriptive for sparse vegetation covering (Ren et al., 2018) as baby-leaf crops are. They have been used for grading wheat powdery mildew disease severity through satellite-acquired scenes (Gröll et al., 2007; Feng et al., 2016; Ma et al., 2018). Recently, SAVI has been applied for the field

estimation of the severity of cotton root rot caused by the fungus *Phymatotrichopsis omnivora* (Zhao et al., 2020), while OSAVI has been used to sense Fusarium Head Blight on wheat by computing Sentinel-2 multispectral data (Liu L. et al., 2020). Similarly to our findings, OSAVI has been found highly correlated with Rhizoctonia crown and root rot severity on sugar beet assessed with a non-imaging remote sensing approach (Reynolds et al., 2012). On the other hand, TVI is the triangular vegetation index associated to leaf chlorophyll content (Cui et al., 2019) and plant vitality (Broge and Leblanc, 2001). It has been calibrated for the leaf area index estimation (Xing et al., 2020) and is also known for describing spectral variations due to wheat leaf rust symptoms caused by *Puccinia triticina* (Ashourloo et al., 2014a,b).

To the best of our knowledge, this is the first study that retrieved hyperspectral VIs with high discriminatory capability for the biocontrol ability of *Trichoderma* against developing soil-borne diseases of leafy vegetables. Previously, Silva et al. (2018)

TABLE 4 | List of the hyperspectral vegetation indices from the literature that were used in this study for estimating their informative degree about disease severity.

Index	Formula	Target	References	Significance on <i>R. solani</i> /Wild rocket	Significance on <i>S. sclerotiorum</i> /Green baby lettuce	Significance on <i>S. rolfsii</i> /Red baby lettuce
AI	Anthocyanin index (AI)	$(R_{600}-R_{699})/(R_{500}-R_{599})$	Anthocyanin	Gamon and Surfus, 1999	ns	ns
ARI	Anthocyanin Reflectance Index (ARI)	$(1/R_{550})-(1/R_{700})$	Carotenoids	Gitelson et al., 2001	ns	****
CAR	Simple ratio 515/570	R_{515}/R_{570}	Carotenoids	Hernández-Clemente et al., 2012	ns	***
DVI	Difference Vegetation Index	$R_{782}-R_{675}$	Plant vitality. Chlorophyll	Tucker, 1979	***	***
FWBI1	Floating-position water band index (FWBI1)	$R_{900}/\min(R_{930}-R_{980})$	Water	Harris et al., 2006	ns	ns
FWBI2	Floating-position water band index (FWBI2)	$R_{920}/\min(R_{960}-R_{1000})$	Water	Harris et al., 2006	ns	ns
G	Simple Ratio 550/670 Greenness Index	R_{550}/R_{670}	Plant vitality. chlorophyll	Smith et al., 1995	***	****
GI	Greenness index	R_{539}/R_{682}	Plant vitality	Zarco-Tejada et al., 2005	***	****
Green-NDVI	Green Normalized Difference Vegetation Index	$(R_{750}-R_{550})/(R_{750}+R_{550})$	Vegetation	Buschmann and Nagel, 1993	ns	ns
HVI	Hyperspectral Vegetation Index	R_{743}/R_{692}	Plant vitality	Gitelson et al., 1996	ns	ns
LIC3	Simple Ratio 440/740 Lichtenthaler indices 3	R_{440}/R_{740}	Carotenoids	Lichtenthaler et al., 1996	ns	ns
LRDSI	Leaf rust disease severity index (LRDSI)	$6.9 \times (R_{605}/R_{455}) - 1.2$	Rust severity	Ashourloo et al., 2014b	ns	****
MCARI	Modified Chlorophyll Absorption in Reflectance Index	$R_{712} \times (R_{712} - R_{682}) - 0.2 \times (R_{712} - R_{539}) / R_{682}$	Chlorophyll	Daughtry, 2000	***	ns
MCARI1	Modified Chlorophyll Absorption in Reflectance Index 1	$1.2 \times [2.5 \times (R_{800} - R_{670}) - 1.3 \times (R_{800} - R_{550})]$	Plant vitality. Chlorophyll	Haboudane, 2004	ns	ns
MSAVI	Modified Soil Adjusted Vegetation Index hyper	$0.5 \times [2 \times R_{800} + 1 - \sqrt{(2 \times R_{800} + 1) \times 2 - 8 \times (R_{800} - R_{670})}]$	Healthy vegetation. Reduces soil noise	Qi et al., 1994	***	***
mSR705	Modified Simple Ratio 705	$(R_{750} - R_{445}) / (R_{705} + R_{445})$	Vegetation	Wu et al., 2008	ns	****
NDVI	Normalized Difference Vegetation Index (NDVI)	$(R_{800} - R_{670}) / (R_{800} + R_{670})$	Plant vitality. Chlorophyll	Rouse et al., 1973	ns	****
NPQI	Normalized Difference 415/435 Normalized Phaeophytinization Index	$R_{415} - R_{435} / R_{415} + R_{435}$	Vegetation. Chlorophyll. Stress	Barnes et al., 1992	ns	ns
OSAVI	Optimized Soil Adjusted Vegetation Index	$(1 + 0.16) \times (R_{800} - R_{670}) / (R_{800} + R_{670} + 0.16)$	Relatively sparse vegetation	Rondeaux et al., 1996	***	****
PRI	Photochemical reflectance index (PRI)	$(R_{531} - R_{570}) / (R_{531} + R_{570})$	Photochemical activity	Gamon et al., 1992	ns	****
PRI515	Normalized Difference 515/531 Photochemical Reflectance Index 515/531	$(R_{515} - R_{531}) / (R_{515} + R_{531})$	Carotenoids	Hernández-Clemente et al., 2011	***	****
PSSRa	Pigment-specific simple ratio (PSSR)	R_{800}/R_{680}	Chlorophyll a	Blackburn, 1998	***	***
PSSRb	Pigment-specific simple ratio (PSSR)	R_{800}/R_{635}	Chlorophyll b	Blackburn, 1998	ns	ns
PSSRc	Pigment-specific simple ratio (PSSR)	R_{800}/R_{470}	Carotenoids	Blackburn, 1998	ns	***
PVI	Perpendicular Vegetation Index	$(R_{800} - 0.2R_{670} - 0.6) / 1.019$	Vegetation	Wiegand and Hatfield, 1988	ns	ns

(Continued)

TABLE 4 | Continued

Index	Formula	Target	References	Significance on <i>R. solani</i> /Wild rocket	Significance on <i>S. sclerotiorum</i> /Green baby lettuce	Significance on <i>S. rolfsii</i> /Red baby lettuce	
R705/ (R717+R491)	New vegetation index	$R_{705}/(R_{717}+R_{491})$	Vegetation. Chlorophyll	Tian et al., 2011	ns	***	ns
RARS	Simple Ratio 760/500 Ratio Analysis of Reflectance Spectra	R_{746}/R_{513}	Carotenoids	Chappelle et al., 1992	ns	ns	ns
RDVI	Renormalized Difference Vegetation Index	$(R_{800}-R_{670})/(R_{800}+R_{670})^{0.5}$	Plant vitality. Chlorophyll	Roujean and Breon, 1995	ns	****	ns
Red Edge NDVI	Red Edge Normalized Difference Vegetation Index	$R_{750}-R_{705}/R_{750}+R_{705}$	Vegetation	Gitelson and Merzlyak, 1994	ns	ns	ns
RGRcn	Red green ratio chlorophyll content (RGRcn)	$(R_{612}+R_{660})/(R_{510}+R_{560})$	Chlorophyll content	Steddom et al., 2003	ns	****	ns
RVI	Ratio vegetation index (RVI)	R_{493}/R_{678}	Plant vitality	Tilley et al., 2003	ns	****	ns
RVSI	Red-Edge Stress Vegetation Index	$R_{800}-R_{670}/(R_{800}+R_{670})0.5$	Plant vitality	Roujean and Breon, 1995	ns	****	ns
SAVI	Soil Adjustment Vegetation Index	$((R_{782}-R_{675})/(R_{782}+R_{675}+0.2))$ (1.2)	Crop Parameters	Baret and Guyot, 1991	***	****	***
SIPI	Structure Intensive Pigment Index 1	$R_{800}-R_{445}/R_{800}/R_{680}$	Vegetation. Chlorophyll	Peñuelas et al., 1995	ns	***	ns
SRI	Simple Ratio Index	R_{800}/R_{680}	Vegetation. Chlorophyll. Leaf area index	Jordan, 1969	***	***	ns
SRPI	Simple Ratio Pigment Index (SRPI)	R_{430}/R_{680}	Vegetation. Chlorophyll	Peñuelas et al., 1994	***	ns	ns
TCARI	Transformed Chlorophyll Absorbance Ratio	$3 \times [(R_{700}-R_{670})-0.2 \times (R_{700}-R_{550}) \times R_{700}/R_{670}]$	Plant vitality. Chlorophyll	Haboudane et al., 2002	ns	****	ns
TSAVI	Transformed Soil Adjustment Vegetation Index	$R_{782}-R_{675}$	Crop Parameters	Baret and Guyot, 1991	***	****	***
TVI	Triangular Vegetation Index	$0.5 \times [120 \times (R_{750}-R_{550})-200 \times (R_{670}-R_{550})]$	Plant vitality. Chlorophyll	Broge and Leblanc, 2001	***	****	***
VARIGreen	Visible atmospherically resistant index (VARIGreen)	$(R_{Green}-R_{Red})/(R_{Green}+R_{Red}-R_{Blue})$	Vegetation	Gitelson et al., 2002	ns	****	ns
VOG1	Simple Ratio 740/720	R_{740}/R_{720}	Plant vitality. Chlorophyll	Vogelmann et al., 1993	ns	ns	ns
VOG2	Simple Ratio 734/747 Vogelmann indices	$(R_{734}-R_{747})/(R_{715}+R_{726})$	Plant vitality. Chlorophyll	Vogelmann et al., 1993	ns	ns	***
VOG3	Simple Ratio 734/747 Vogelmann indices 3	$(R_{734}-R_{747})/(R_{715}+R_{720})$	Plant vitality. Chlorophyll	Vogelmann et al., 1993	ns	ns	***
WBI	Water band index (WBI)	R_{950}/R_{900}	Water	Peñuelas et al., 1993	ns	ns	ns
WI	Water Index	R_{900}/R_{970}	Water	Peñuelas et al., 1997	ns	ns	ns
ZTM	Zarco - Tejada - Miller Index	R_{750}/R_{710}	Chlorophyll	Zarco-Tejada et al., 2001	ns	ns	ns

For each one the formula, functional target, literature reference and the significance level (ns: $P > 0.05$; * $P \leq 0.05$; ** $P \leq 0.01$; *** $P \leq 0.001$; **** $P \leq 0.0001$) of the cross-correlation with disease severity index for the three different pathosystems were reported.

have tried to apply a laser speckle based on a light signal at 632 nm to assess the efficacy of maize seed treatments with *T. harzianum* on the germination, vigor and sanitation of seedlings. Instead, Pishchik et al. (2016) have calculated VIs on VIS, RED (red-edge), NIR and MID (middle infrared) spectral information acquired with a field pulse photometer, to tentatively track the synergistic effect of the plant growth promoting bacteria,

Bacillus subtilis and a humic fertilizer on lettuce plants quality and vitality.

The four indices of this study, each applying its own peculiar algorithm, work in the spectral range 550–800 nm, just on the border between VIS and NIR regions, suggesting that this part of the spectrum could be sensitive to the reflectance shifts occurring at canopy level during the plant-pathogen-antagonist interaction.

Marín-Ortiz et al. (2020) have found in the VIS/NIR range 448–995 nm the distinctive spectral response of tomato to the *Fusarium oxysporum* infection that has been also associated to changes in the leaf concentration of chlorophyll and carotene. Similarly, the soil-borne pathogens studied in our systems could bring to the decline of chlorophyll and other pigments, as-well-as growth reduction conditioning the reflectance reaction.

As a matter of fact, decreases in chlorophyll content has been noticed in Rhizoctonia diseased carrot (Ahmad et al., 2019), in cucumber affected both by *R. solani* and *S. rolfisii* (Kotasthane et al., 2015) and in soybean attacked by *S. sclerotiorum* (Vitorino et al., 2020). On the contrary, *Trichoderma* can enhance the photosynthetic performances of the colonized plants by increasing their chlorophyll content and, at the same time, determining an improvement of their general physiological status (Singh et al., 2013; Doley et al., 2014; Kotasthane et al., 2015) exerting an antagonistic action with respect to the pathogen in promoting the vitality of the plant. Therefore, according to these inferences the plant functional imaging as applied here may return valuable information about how the biocontrol agents is working.

Findings of the present study indicate the potential to boost the sustainability of disease management protocols through high-performing hyperspectral VIs that can drive the biocontrol practices, such as, for example, the microbial augmentation, based on the early recognition of the worsening of the plant state and of the possible effectiveness reduction of the adopted plant protection strategy. Functional plant imaging can be used to track the plant progression under biocontrol effect using a restricted number of bands. The digital imaging has been proposed for the early diagnosis of plant diseases (Lowe et al., 2017), for the real-time field estimation of phytopathological conditions (Golhani et al., 2018) and to provide useful information for pest and disease control (Yao et al., 2011). Here, it helped to scout effective biological control agents against baby-leaf salad pathogens, demonstrating the potential to sense the biocontrol making on developing soil-borne diseases. The association between BCAs and hyperspectral imaging, concurring at reducing chemical pressure of fungicides on the environment and avoiding crop losses for uncontrolled pathogenic attacks, opens to the concept of precision biological control. The availability of digital tools for the automatized large-scale evaluation of biocontrol evolution will be useful both in field/greenhouse systems to rapidly assess the success of biological measures against phytopathogens as well as Susič et al. (2020) have recently pointed up for pest control.

CONCLUSIONS

The high-effective *Trichoderma* strains identified in this study are able for protecting baby-leaf vegetables from a wide-spectrum of soil-borne pathogens, such as *R. solani*, *S. sclerotiorum*, and *R. rolfisii*. Strains belonging to *T. longibrachiatum*, *T. atroviride*, and *T. harzianum* are suitable for large-scale preventive applications in greenhouses that host wild rocket and baby-lettuces in succession and/or in rotation and have

a perspective to work in consortia since they sourced from a unique niche. The scenario of applying digital imaging as innovative scheme to boost biological control, from the high throughput screening of the microorganisms to their field application, is highlighted. OSAVI, SAVI, TSAVI, and TVI, that were found highly correlated to disease severity, are promising and informative hyperspectral VIs to track biological control activity against multiple soil-borne pathogens of baby leaf vegetables. In future studies, digital imaging will be able to integrate metabolomic linked to transcriptomic analyses, which, supported by machine learning processing, can contribute to further improve the accuracy of the forecasting models by imaging applied to the plant protection practices.

DATA AVAILABILITY STATEMENT

The datasets presented in this study can be found in online repositories. The names of the repository/repositories and accession number(s) can be found below: <https://www.ncbi.nlm.nih.gov/genbank/>, MW191738; <https://www.ncbi.nlm.nih.gov/genbank/>, MW191739; <https://www.ncbi.nlm.nih.gov/genbank/>, MW191740; <https://www.ncbi.nlm.nih.gov/genbank/>, MW191741; <https://www.ncbi.nlm.nih.gov/genbank/>, MW191742; <https://www.ncbi.nlm.nih.gov/genbank/>, MW191743; <https://www.ncbi.nlm.nih.gov/genbank/>, MW191744; <https://www.ncbi.nlm.nih.gov/genbank/>, MW191751; <https://www.ncbi.nlm.nih.gov/genbank/>, MW191737; <https://www.ncbi.nlm.nih.gov/genbank/>, MW191745; <https://www.ncbi.nlm.nih.gov/genbank/>, MW191747; <https://www.ncbi.nlm.nih.gov/genbank/>, MW191746; <https://www.ncbi.nlm.nih.gov/genbank/>, MW191749; <https://www.ncbi.nlm.nih.gov/genbank/>, MW191750; <https://www.ncbi.nlm.nih.gov/genbank/>, MW191748; <https://www.ncbi.nlm.nih.gov/genbank/>, MW191752; <https://www.ncbi.nlm.nih.gov/genbank/>, MW201694; <https://www.ncbi.nlm.nih.gov/genbank/>, MW201695; <https://www.ncbi.nlm.nih.gov/genbank/>, MW201689; <https://www.ncbi.nlm.nih.gov/genbank/>, MW201690; <https://www.ncbi.nlm.nih.gov/genbank/>, MW201692; <https://www.ncbi.nlm.nih.gov/genbank/>, MW201693; <https://www.ncbi.nlm.nih.gov/genbank/>, MW201691; <https://www.ncbi.nlm.nih.gov/genbank/>, MW201701; <https://www.ncbi.nlm.nih.gov/genbank/>, MW201688; <https://www.ncbi.nlm.nih.gov/genbank/>, MW201697; <https://www.ncbi.nlm.nih.gov/genbank/>, MW201696; <https://www.ncbi.nlm.nih.gov/genbank/>, MW201699; <https://www.ncbi.nlm.nih.gov/genbank/>, MW201700; <https://www.ncbi.nlm.nih.gov/genbank/>, MW201698; <https://www.ncbi.nlm.nih.gov/genbank/>, MW201702; <https://www.ncbi.nlm.nih.gov/genbank/>, MW246311.

AUTHOR CONTRIBUTIONS

GM and CP conceived and designed the study and wrote the initial manuscript. GM, NN, MC, and CP conducted the experiments. GM and NN analyzed data. CP assisted in data

analysis and interpretation of results. MZ and TC reviewed and edited the final version of the manuscript. All authors have read and agreed to the published version of the manuscript.

FUNDING

This research was funded by the Italian Ministry of Agriculture, Food and Forestry Policies (MiPAAF), project AgriDigit, sub-project Tecnologie digitali integrate per il

rafforzamento sostenibile di produzioni e trasformazioni agroalimentari (AgroFiliere) (DM 36503.7305.2018 of 20/12/2018).

ACKNOWLEDGMENTS

The authors are grateful to Diana Perrotti and Stefano Guarracino for the graphical support about the representation of hyperspectral images.

REFERENCES

- Ahmad, L., Siddiqui, Z. A., and Abd_Allah, E. F. (2019). Effects of interaction of *Meloidogyne incognita*, *Alternaria dauci* and *Rhizoctonia solani* on the growth, chlorophyll, carotenoid and proline contents of carrot in three types of soil. *Acta Agric. Scand. B Soil Plant Sci.* 69, 1–8. doi: 10.1080/09064710.2019.1568541
- Anderberg, M. R. (1973). *Cluster Analysis for Applications*. New York, NY; London: Academic Press.
- Ashourloo, D., Mobasheri, M., and Huete, A. (2014a). Evaluating the effect of different wheat rust disease symptoms on vegetation indices using hyperspectral measurements. *Remote Sens.* 6, 5107–5123. doi: 10.3390/rs6065107
- Ashourloo, D., Mobasheri, M. R., and Huete, A. (2014b). Developing two spectral disease indices for detection of wheat leaf rust (*Puccinia triticina*). *Remote Sens.* 6, 4723–4740. doi: 10.3390/rs6064723
- Baret, F., and Guyot, G. (1991). Potentials and limits of vegetation indices for LAI and APAR assessment. *Remote Sens. Environ.* 35, 161–173. doi: 10.1016/0034-4257(91)90009-U
- Barnes, J. D., Balaguer, L., Manrique, E., Elvira, S., and Davison, A. W. (1992). A reappraisal of the use of DMSO for the extraction and determination of chlorophylls a and b in lichens and higher plants. *Environ. Exp. Bot.* 32, 85–100. doi: 10.1016/0098-8472(92)90034-Y
- Bastakoti, S., Belbase, S., Manandhar, S., and Arjyal, C. (2017). *Trichoderma* species as biocontrol agent against soil borne fungal pathogens. *Nepal J. Biotechnol.* 5:39. doi: 10.3126/njb.v5i1.18492
- Blackburn, G. A. (1998). Quantifying chlorophylls and carotenoids at leaf and canopy scales. *Remote Sens. Environ.* 66, 273–285. doi: 10.1016/S0034-4257(98)00059-5
- Bonini, P., Roupael, Y., Cardarelli, M., Ceccarelli, A. V., and Colla, G. (2020). Effectiveness of *Trichoderma* application through drip-irrigation to reduce *Sclerotinia* disease incidence and improve the growth performance of greenhouse lettuce. *Acta Hort.* 1268, 199–204. doi: 10.17660/ActaHortic.2020.1268.26
- Bonnarme, P., Djian, A., Latrasse, A., Féron, G., Giniès, C., Durand, A., et al. (1997). Production of 6-pentyl- α -pyrone by *Trichoderma* sp. from vegetable oils. *J. Biotechnol.* 56, 143–150. doi: 10.1016/S0168-1656(97)00108-9
- Broge, N. H., and Leblanc, E. (2001). Comparing prediction power and stability of broadband and hyperspectral vegetation indices for estimation of green leaf area index and canopy chlorophyll density. *Remote Sens. Environ.* 76, 156–172. doi: 10.1016/S0034-4257(00)00197-8
- Buschmann, C., and Nagel, E. (1993). *In vivo* spectroscopy and internal optics of leaves as basis for remote sensing of vegetation. *Int. J. Remote Sens.* 14, 711–722. doi: 10.1080/01431169308904370
- Caruso, G., El-Nakhel, C., Roupael, Y., Comite, E., Lombardi, N., Cuciniello, A., et al. (2020). *Diplotaxis tenuifolia* (L.) DC. Yield and quality as influenced by cropping season, protein hydrolysates, and trichoderma applications. *Plants* 9:697. doi: 10.3390/plants9060697
- Caruso, G., Parrella, G., Giorgini, M., and Nicoletti, R. (2018). Crop systems, quality and protection of *Diplotaxis tenuifolia*. *Agriculture* 8:55. doi: 10.3390/agriculture8040055
- Chappelle, E. W., Kim, M. S., and McMurtrey, J. E. (1992). Ratio analysis of reflectance spectra (RARS): an algorithm for the remote estimation of the concentrations of chlorophyll a, chlorophyll b, and carotenoids in soybean leaves. *Remote Sens. Environ.* 39, 239–247. doi: 10.1016/0034-4257(92)90089-3
- Chilosi, G., Aleandri, M. P., Luccioli, E., Stazi, S. R., Marabottini, R., Morales-Rodríguez, C., et al. (2020). Suppression of soil-borne plant pathogens in growing media amended with espresso spent coffee grounds as a carrier of *Trichoderma* spp. *Sci. Hortic.* 259:108666. doi: 10.1016/j.scienta.2019.108666
- Cui, B., Zhao, Q., Huang, W., Song, X., Ye, H., and Zhou, X. (2019). A new integrated vegetation index for the estimation of winter wheat leaf chlorophyll content. *Remote Sens.* 11:974. doi: 10.3390/rs11080974
- da Silva, G. B. P., Heckler, L. I., Durigon, M., dos Santos, R. F., Lovato, M., Finger, G., et al. (2019). Biological control of white mold (*Sclerotinia sclerotiorum*) in lettuce using Brazilian *Trichoderma* spp. strains. *Aust. J. Crop Sci.* 13, 803–809. doi: 10.21475/ajcs.19.13.06.p1214
- da Silva, L. R., Valadares-Ingles, M. C., Peixoto, G. H. S., Gonçalves deLuccas, B. E., CostaMuniz, P. H. P., Martins Magalhães, D., et al. (2021). Volatile organic compounds emitted by *Trichoderma azevedoi* promote the growth of lettuce plants and delay the symptoms of white mold. *Biol. Control.* 152:104447. doi: 10.1016/j.biocontrol.2020.104447
- Darvin, G. (2013). Effect of plant extracts on radial growth of *Sclerotium rolfsii* Sacc. causing stem rot of groundnut. *Int. J. Appl. Biol. Pharm. Technol.* 4, 69–73.
- Daughtry, C. (2000). Estimating corn leaf chlorophyll concentration from leaf and canopy reflectance. *Remote Sens. Environ.* 74, 229–239. doi: 10.1016/S0034-4257(00)00113-9
- Di Mola, I., Ottaiano, L., Cozzolino, E., Senatore, M., Sacco, A., El-Nakhel, C., et al. (2020). *Trichoderma* spp. and mulching films differentially boost qualitative and quantitative aspects of greenhouse lettuce under diverse N conditions. *Horticulturae* 6:55. doi: 10.3390/horticulturae6030055
- Doley, K., Dudhane, M., Borde, M., and Jite, P. (2014). Effects of *Glomus fasciculatum* and *Trichoderma asperelloides* in roots of groundnut (Cv. Western-51) against pathogen *Sclerotium rolfsii*. *Int. J. Phytopathol.* 3, 89–100. doi: 10.33687/phytopath.003.02.0809
- El Enshasy, H. A., Ambehatabi, K. K., El Baz, A. F., Ramchuran, S., Sayyed, R. Z., Amalin, D., et al. (2020). “*Trichoderma*: biocontrol agents for promoting plant growth and soil health,” in *Agriculturally Important Fungi for Sustainable Agriculture*, eds A. Yadav, S. Mishra, D. Kour, N. Yadav, A. Kumar (Cham: Springer), 239–259. doi: 10.1007/978-3-030-48474-3_8
- Elias, L. M., Domingues, M. V. P., Moura, K. E. D., Harakava, R., and Patricio, F. R. A. (2016). Selection of *Trichoderma* isolates for biological control of *Sclerotinia minor* and *S. sclerotiorum* in lettuce. *Summa Phytopathol.* 42, 216–221. doi: 10.1590/0100-5405/2147
- Feng, W., Shen, W., He, L., Duan, J., Guo, B., Li, Y., et al. (2016). Improved remote sensing detection of wheat powdery mildew using dual-green vegetation indices. *Precis. Agric.* 17, 608–627. doi: 10.1007/s11119-016-9440-2
- Fiorentino, N., Ventrino, V., Woo, S. L., Pepe, O., De Rosa, A., Gioia, L., et al. (2018). *Trichoderma*-based biostimulants modulate rhizosphere microbial populations and improve n uptake efficiency, yield, and nutritional quality of leafy vegetables. *Front. Plant Sci.* 9:743. doi: 10.3389/fpls.2018.00743
- Gamon, J. A., Peñuelas, J., and Field, C. B. (1992). A narrow-waveband spectral index that tracks diurnal changes in photosynthetic efficiency. *Remote Sens. Environ.* 41, 35–44. doi: 10.1016/0034-4257(92)90059-S
- Gamon, J. A., and Surfus, J. S. (1999). Assessing leaf pigment content and activity with a reflectometer. *New Phytol.* 143, 105–117. doi: 10.1046/j.1469-8137.1999.00424.x

- Gardes, M., and Bruns, T. D. (1993). ITS primers with enhanced specificity for basidiomycetes—application to the identification of mycorrhizae and rusts. *Mol. Ecol.* 2, 113–118. doi: 10.1111/j.1365-294X.1993.tb00005.x
- Gilardi, G., Gullino, M. L., and Garibaldi, A. (2018a). Emerging foliar and soil-borne pathogens of leafy vegetable crops: a possible threat to Europe. *EPP0 Bull.* 48, 116–127. doi: 10.1111/epp.12447
- Gilardi, G., Gullino, M. L., and Garibaldi, A. (2018b). Emerging soil-borne and foliar diseases on leafy vegetables for fresh-cut production in northern Italy. *Acta Hort.* 1209, 65–70. doi: 10.17660/ActaHortic.2018.1209.10
- Giménez, A., Fernández, J. A., Pascual, J. A., Ros, M., López-Serrano, M., and Egea-Gilbert, C. (2019). An agroindustrial compost as alternative to peat for production of baby leaf red lettuce in a floating system. *Sci. Hortic.* 246, 907–915. doi: 10.1016/j.scienta.2018.11.080
- Gitelson, A., and Merzlyak, M. N. (1994). Quantitative estimation of chlorophyll-a using reflectance spectra: experiments with autumn chestnut and maple leaves. *J. Photochem. Photobiol. B. Biol.* 22, 247–252. doi: 10.1016/1011-1344(93)06963-4
- Gitelson, A. A., Kaufman, Y. J., Stark, R., and Rundquist, D. (2002). Novel algorithms for remote estimation of vegetation fraction. *Remote Sens. Environ.* 80, 76–87. doi: 10.1016/S0034-4257(01)00289-9
- Gitelson, A. A., and Merzlyak, M. N., Chivkunova, O. B. (2001). Optical properties and nondestructive estimation of anthocyanin content in plant leaves. *Photochem. Photobiol.* 74:38. doi: 10.1562/0031-8655(2001)074andlt;0038:OPANEOandgt;2.0.CO;2
- Gitelson, A. A., Merzlyak, M. N., and Lichtenthaler, H. K. (1996). Detection of red edge position and chlorophyll content by reflectance measurements near 700 nm. *J. Plant Physiol.* 148, 501–508. doi: 10.1016/S0176-1617(96)80285-9
- Golhani, K., Balasundram, S. K., Vadmalai, G., and Pradhan, B. (2018). A review of neural networks in plant disease detection using hyperspectral data. *Inf. Process. Agric.* 5, 354–371. doi: 10.1016/j.inpa.2018.05.002
- Gröll, K., Graeff, S., and Claupein, W. (2007). “Use of vegetation indices to detect plant diseases,” in *Agrarinformatik im Spannungsfeld zwischen Regionalisierung und globalen Wertschöpfungsketten – Referate der 27. GIL Jahrestagung*, eds S. Böttinger, L. Theuvsen, S. Rank, and M. Morgenstern (Bonn: Gesellschaft für Informatik e. V.), 91–94.
- Gullino, M. L., Gilardi, G., and Garibaldi, A. (2019). Ready-to-eat salad crops: a plant pathogen's heaven. *Plant Dis.* 103:9. doi: 10.1094/PDIS-03-19-0472-FE
- Haboudane, D. (2004). Hyperspectral vegetation indices and novel algorithms for predicting green LAI of crop canopies: modeling and validation in the context of precision agriculture. *Remote Sens. Environ.* 90, 337–352. doi: 10.1016/j.rse.2003.12.013
- Haboudane, D., Miller, J. R., Tremblay, N., Zarco-Tejada, P. J., and Dextraze, L. (2002). Integrated narrow-band vegetation indices for prediction of crop chlorophyll content for application to precision agriculture. *Remote Sens. Environ.* 81, 416–426. doi: 10.1016/S0034-4257(02)00018-4
- Harris, A., Bryant, R. G., and Baird, A. J. (2006). Mapping the effects of water stress on *Sphagnum*: preliminary observations using airborne remote sensing. *Remote Sens. Environ.* 100, 363–378. doi: 10.1016/j.rse.2005.10.024
- Hernández-Clemente, R., Navarro-Cerrillo, R. M., Suárez, L., Morales, F., and Zarco-Tejada, P. J. (2011). Assessing structural effects on PRI for stress detection in conifer forests. *Remote Sens. Environ.* 115, 2360–2375. doi: 10.1016/j.rse.2011.04.036
- Hernández-Clemente, R., Navarro-Cerrillo, R. M., and Zarco-Tejada, P. J. (2012). Carotenoid content estimation in a heterogeneous conifer forest using narrow-band indices and PROSPECT+DART simulations. *Remote Sens. Environ.* 127, 298–315. doi: 10.1016/j.rse.2012.09.014
- Hijmans, R. J., Van Etten, J., Cheng, J., Mattiuzzi, M., Sumner, M., Greenberg, J. A., et al. (2015). Package “raster.” *R Package* 734.
- Hirpara, D. G., Gajera, H. P., Hirpara, H. Z., and Golakiya, B. A. (2017). Antipathy of *Trichoderma* against *Sclerotium rolfsii* Sacc.: evaluation of cell wall-degrading enzymatic activities and molecular diversity analysis of antagonists. *J. Mol. Microbiol. Biotechnol.* 27, 22–28. doi: 10.1159/000452997
- Howell, C. R. (2003). Mechanisms employed by *Trichoderma* species in the biological control of plant diseases: the history and evolution of current concepts. *Plant Dis.* 87, 4–10. doi: 10.1094/PDIS.2003.87.1.4
- Jones, E. E., Stewart, A., and Whipps, J. M. (2003). Use of *Coniothyrium minitans* transformed with the hygromycin B resistance gene to study survival and infection of *Sclerotinia sclerotiorum* sclerotia in soil. *Mycol. Res.* 107, 267–276. doi: 10.1017/S0953756203007457
- Jordan, C. F. (1969). Derivation of leaf-area index from quality of light on the forest floor. *Ecology* 50, 663–666. doi: 10.2307/1936256
- Kareem, T. K., Ugoji, O. E., and Aboaba, O. O. (2016). Biocontrol of *Fusarium* wilt of cucumber with *Trichoderma longibrachiatum* NGJ167 (Rifai). *Br. Microbiol. Res. J.* 16, 1–11. doi: 10.9734/BMRJ/2016/28208
- Kassambara, A., and Mundt, F. (2017). *Package “Factoextra.” Extract and Visualize the Results of Multivariate Data Analyses.* 76.
- Kotasthane, A., Agrawal, T., Kushwah, R., and Rahatkar, O. V. (2015). *In-vitro* antagonism of *Trichoderma* spp. against *Sclerotium rolfsii* and *Rhizoctonia solani* and their response towards growth of cucumber, bottle gourd and bitter melon. *Eu. J. Plant Pathol.* 141, 523–543. doi: 10.1007/s10658-014-0560-0
- Kumar, G., Maharshi, A., Patel, J., Mukherjee, A., Singh, H. B., and Sarma, B. K. (2017). *Trichoderma*: a potential fungal antagonist to control plant diseases. *SATSA Mukhapatra Annu. Tech. Issue* 21:206.
- Kumar, S., Stecher, G., and Tamura, K. (2016). MEGA7: molecular evolutionary genetics analysis version 7.0 for bigger datasets. *Mol. Biol. Evol.* 33, 1870–1874. doi: 10.1093/molbev/msw054
- Larkin, R. P., and Honeycutt, C. W. (2006). Effects of different 3-year cropping systems on soil microbial communities and *Rhizoctonia* diseases of potato. *Phytopathology* 96, 68–79. doi: 10.1094/PHYTO-96-0068
- Lichtenthaler, H. K., Lang, M., Sowinska, M., Heisel, F., and Miehe, J. A. (1996). Detection of vegetation stress via a new high resolution fluorescence imaging system. *J. Plant Physiol.* 148, 599–612. doi: 10.1016/S0176-1617(96)80081-2
- Liu, H., Bruning, B., Garnett, T., and Berger, B. (2020). Hyperspectral imaging and 3D technologies for plant phenotyping: from satellite to close-range sensing. *Comput. Electron. Agr.* 175:105621. doi: 10.1016/j.compag.2020.105621
- Liu, L., Dong, Y., Huang, W., Du, X., Ren, B., Huang, L., et al. (2020). Wheat fusarium head blight using sentinel-2 multispectral imagery. *IEEE Access.* 8, 52181–52191. doi: 10.1109/ACCESS.2020.2980310
- Longo, M. A., and Sanromán, M. N. (2006). Production of food aroma compounds: microbial and enzymatic methodologies. *Food Technol. Biotechnol.* 44, 335–353. doi: 10.1201/9780429441837-15
- Lowe, A., Harrison, N., and French, A. P. (2017). Hyperspectral image analysis techniques for the detection and classification of the early onset of plant disease and stress. *Plant Methods.* 13:80. doi: 10.1186/s13007-017-0233-z
- Ma, H., Jing, Y., Huang, W., Shi, Y., Dong, Y., Zhang, J., et al. (2018). Integrating early growth information to monitor winter wheat powdery mildew using multi-temporal landsat-8 imagery. *Sensors* 18:3290. doi: 10.3390/s18103290
- MacQueen, J. B. (1967). Some methods for classification and analysis of multivariate observations. *Proc. Berkeley Symp. Math. Statist. Prob.* 1, 281–297.
- Marín-Ortiz, J. C., Gutierrez-Toro, N., Botero-Fernández, V., and Hoyos-Carvajal, L. M. (2020). Linking physiological parameters with visible/near-infrared leaf reflectance in the incubation period of vascular wilt disease. *Saudi J. Biol. Sci.* 27, 88–99. doi: 10.1016/j.sjbs.2019.05.007
- Marques, E., Martins, I., and de Mello, S. C. M. (2018). Antifungal potential of crude extracts of *Trichoderma* spp. *Biota Neotrop.* 18:e20170418. doi: 10.1590/1676-0611-bn-2017-0418
- Martins, L. M., Neiro, E., da, S., Dias, A. R., Roque, C. G., Rojo Baio, F. H., et al. (2018). Cotton vegetation indices under different control methods of ramularia leaf spot. *Biosci. J.* 34, 1706–1713. doi: 10.14393/BJ-v34n6a2018-39975
- Mishra, P., Asari, M. S. M., Herrero-Langreo, A., Lohumi, S., Diezma, B., and Scheunders, P. (2017). Close range hyperspectral imaging of plants: a review. *Biosyst. Eng.* 164, 49–67. doi: 10.1016/j.biosystemseng.2017.09.009
- Morra, L., Cerrato, D., Bilotto, M., and Baiano, S. (2017). Introduction of sorghum [*Sorghum bicolor* (L.) Moench] green manure in rotations of head salads and baby leaf crops under greenhouse. *Ital. J. Agron.* 12:753. doi: 10.4081/ija.2016.753
- Nicoletti, R., Raimo, F., and Miccio, G. (2004). First report of *Rhizoctonia solani* on *Diplotaxis tenuifolia* in Italy. *Plant Pathol.* 53, 811–811. doi: 10.1111/j.1365-3059.2004.01078.x
- Nicoletti, R., Raimo, F., and Miccio, G. (2007). *Diplotaxis tenuifolia*: biology, production and properties. *Eur. J. Plant Sci. Biotechnol.* 1, 36–43.
- O'Donnell, K., Kistler, H. C., Cigelnik, E., and Plötz, R. C. (1998). Multiple evolutionary origins of the fungus causing Panama disease of banana:

- concordant evidence from nuclear and mitochondrial gene genealogies. *Proc. Natl. Acad. Sci.* 95, 2044–2049 doi: 10.1073/pnas.95.5.2044
- Ospina-Giraldo, M. D., Royse, D. J., Chen, X., and Romaine, C. P. (1999). Molecular phylogenetic analyses of biological control strains of *Trichoderma harzianum* and other biotypes of *Trichoderma* spp. associated with mushroom green mold. *Phytopathology* 89, 308–313. doi: 10.1094/PHYTO.1999.89.4.308
- Pane, C., Sigillo, L., Caputo, M., Serratore, G., Zaccardelli, M., and Tripodi, P. (2017). Response of rocket salad germplasm (*Eruca* and *Diplotaxis* spp.) to major pathogens causing damping-off, wilting and leaf spot diseases. *Arch. Phytopathol. Pflanzenschutz*. 50, 167–177. doi: 10.1080/03235408.2017.1285511
- Pane, C., Sorrentino, R., Scotti, R., Molisso, M., Di Matteo, A., Celano, G., et al. (2020). Alpha and beta-diversity of microbial communities associated to plant disease suppressive functions of on-farm green composts. *Agriculture* 10:113. doi: 10.3390/agriculture10040113
- Pañitur-De la Fuente, C., Valdés-Gómez, H., Roudet, J., Verdugo-Vásquez, N., Mirabal, Y., Laurie, V. F., et al. (2020). Vigor thresholded NDVI is a key early risk indicator of Botrytis bunch rot in vineyards. *OENO One* 52, 279–297. doi: 10.20870/oeno-one.2020.54.2.2954
- Pascale, A., Vinale, F., Manganiello, G., Nigro, M., Lanzuise, S., Ruocco, M., et al. (2017). *Trichoderma* and its secondary metabolites improve yield and quality of grapes. *Crop Prot.* 92, 176–181. doi: 10.1016/j.cropro.2016.11.010
- Patterson, C. L., and Grogan, R. G. (1985). Differences in epidemiology and control of lettuce drop caused by *Sclerotinia minor* and *S. sclerotiorum*. *Plant Dis.* 69, 766–770. doi: 10.1094/PD-69-766
- Penha, M. P., Rocha-Leao, M. H. M., and Leite, S. G. F. (2012). Sugarcane bagasse as support for the production of coconut aroma by solid-state fermentation (SSF). *Bioresources* 7, 2366–2375. doi: 10.15376/biores.7.2.2366-2375
- Peñuelas, J., Baret, F., and Filella, I. (1995). Semi-empirical indices to assess carotenoids/chlorophyll-a ratio from leaf spectral reflectance. *Photosynthetica* 31, 221–230.
- Peñuelas, J., Filella, I., Briel, C., Serrano, L., and Savé R. (1993). The reflectance at the 950–970 nm region as an indicator of plant water status. *Int. J. Remote Sens.* 14, 1887–1905. doi: 10.1080/01431169308954010
- Peñuelas, J., Gamon, J. A., Fredeen, A. L., Merino, J., and Field, C. B. (1994). Reflectance indices associated with physiological changes in nitrogen- and water-limited sunflower leaves. *Remote Sens. Environ.* 48, 135–146. doi: 10.1016/0034-4257(94)90136-8
- Peñuelas, J., Pinol, J., Ogaya, R., and Filella, I. (1997). Estimation of plant water concentration by the reflectance water index WI (R900/R970). *Int. J. Remote Sens.* 18, 2869–2875. doi: 10.1080/014311697217396
- Phillips, A. J. L. (1989). Fungi associated with sclerotia of *Sclerotinia sclerotiorum* in South Africa and their effects on the pathogen. *Phytophylactica* 21, 135–140.
- Pishchik, V. N., Vorobyov, N. I., Walsh, O. S., Surin, V. G., and Khomyakov, Y. V. (2016). Estimation of synergistic effect of humic fertilizer and *Bacillus subtilis* on lettuce plants by reflectance measurements. *J. Plant Nutr.* 39, 1074–1086. doi: 10.1080/01904167.2015.1061551
- Qi, J., Chehbouni, A., Huete, A. R., Kerr, Y. H., and Sorooshian, S. (1994). A modified soil adjusted vegetation index. *Remote Sens. Environ.* 48, 119–126. doi: 10.1016/0034-4257(94)90134-1
- Ramos, A. S., Fiaux, S. B., and Leite, S. G. F. (2008). Production of 6-pentyl- α -pyrone by *Trichoderma harzianum* in solid-state fermentation. *Braz. J. Microbiol.* 39, 712–717. doi: 10.1590/S1517-83822008000400022
- Ren, H., Zhou, G., and Zhang, F. (2018). Using negative soil adjustment factor in soil-adjusted vegetation index (SAVI) for aboveground living biomass estimation in arid grasslands. *Remote Sens. Environ.* 209, 439–445. doi: 10.1016/j.rse.2018.02.068
- Reynolds, G. J., Windels, C. E., MacRae, I. V., and Laguette, S. (2012). Remote sensing for assessing Rhizoctonia crown and root rot severity in sugar beet. *Plant Dis.* 96, 497–505. doi: 10.1094/PDIS-11-10-0831
- Rondeaux, G., Steven, M., and Baret, F. (1996). Optimization of soil-adjusted vegetation indices. *Remote Sens. Environ.* 55, 95–107. doi: 10.1016/0034-4257(95)00186-7
- Roujean, J.-L., and Breon, F.-M. (1995). Estimating PAR absorbed by vegetation from bidirectional reflectance measurements. *Remote Sens. Environ.* 51, 375–384. doi: 10.1016/0034-4257(94)00114-3
- Rouphael, Y., Carillo, P., Colla, G., Fiorentino, N., Sabatino, L., El-Nakhel, C., et al. (2020). Appraisal of combined applications of *Trichoderma virens* and a biopolymer-based biostimulant on lettuce agronomical, physiological, and qualitative properties under variable N regimes. *Agronomy* 10:196. doi: 10.3390/agronomy10020196
- Rouse, J. Jr., Haas, R., Schell, J., and Deering, D. (1973). “Monitoring vegetation systems in the Great Plains with ERTS,” in *Proceedings of the Third Earth Resources Technology Satellite-1 Symposium* (Washington, DC).
- Sachdev, S., and Singh, R. P. (2020). “Trichoderma: a multifaceted fungus for sustainable agriculture”, in *Ecological and Practical Applications for Sustainable Agriculture*, eds K. Baudhdh, S. Kumar, R. Singh, and J. Korstad (Singapore: Springer), 261–304. doi: 10.1007/978-981-15-3372-3_13
- Samuels, G. J., Ismael, A., Bon, M. C., De Respíns, S., and Petrini, O. (2010). *Trichoderma asperellum* sensu lato consists of two cryptic species. *Mycologia* 102, 944–966. doi: 10.3852/09-243
- Saxena, D., Tewari, A. K., and Rai, D. (2014). *In vitro* antagonistic assessment of *T. harzianum* PBT 23 against plant pathogenic fungi. *J. Microbiol. Biotechnol. Res.* 4, 59–65.
- Schlatter, D., Kinkel, L., Thomashow, L., Weller, D., and Paulitz, T. (2017). Disease suppressive soils: new insights from the soil microbiome. *Phytopathology* 107, 1284–1297. doi: 10.1094/PHYTO-03-17-0111-RVW
- Schroers, H. J., Samuels, G. J., Seifert, K. A., and Gams, W. (1999). Classification of the mycoparasite *Gliocladium roseum* in *Clonostachys* as *C. rosea*, its relationship to *Bionectria ochroleuca*, and notes on other *Gliocladium*-like fungi. *Mycologia* 91, 365–385 doi: 10.1080/00275514.1999.12061028
- Scotti, R., Mitchell, A. L., Pane, C., Finn, R. D., and Zaccardelli, M. (2020). Microbiota characterization of agricultural green waste-based suppressive composts using omics and classic approaches. *Agriculture* 10:61. doi: 10.3390/agriculture10030061
- Serrano-Carreón, L., Flores, C., Rodríguez, B., and Galindo, E. (2004). *Rhizoctonia solani*, an elicitor of 6-pentyl- α -pyrone production by *Trichoderma harzianum* in a two liquid phases, extractive fermentation system. *Biotechnol. Lett.* 26, 1403–1406. doi: 10.1023/B:BILE.0000045640.71840.b5
- Sharma, S., Kour, D., Rana, K. L., Dhiman, A., Thakur, S., Thakur, P., et al. (2019). “Trichoderma: biodiversity, ecological significances, and industrial applications” in *Recent Advancement in White Biotechnology through Fungi*, eds A. Yadav, S. Mishra, S. Singh, and A. Gupta (Cham: Springer), 85–120 doi: 10.1007/978-3-030-10480-1_3
- Silva, G. M., Peixoto, L. S., Fujii, A. K., Parisi, J. J. D., Aguiar, R. H., and Fracarolli, J. A. (2018). Evaluation of maize seeds treated with *Trichoderma*® through biospeckle. *J. Agr. Sci. Tech-IRAN.* 8, 175–187. doi: 10.17265/2161-6264/2018.03.004
- Singh, S., Singh, H., Singh, D., Chandra, B., and Viswa, K. (2013). *Trichoderma harzianum* and *Pseudomonas* sp. mediated management of *Sclerotium rolfsii* rot in tomato (*Lycopersicon esculentum* mill.). *Bioscan.* 8, 801–804.
- Smith, R. C. G., Adams, J., Stephens, D. J., and Hick, P. T. (1995). Forecasting wheat yield in a mediterranean-type environment from the NOAA satellite. *Aust. J. Agric. Res.* 46:113. doi: 10.1071/AR950113
- Sridharan, A. P., Thankappan, S., and Karthikeyan, G., Uthandi, S. (2020). Comprehensive profiling of the VOCs of *Trichoderma longibrachiatum* EF5 while interacting with *Sclerotium rolfsii* and *Macrophomina phaseolina*. *Microbiol. Res.* 236, 126–436. doi: 10.1016/j.micres.2020.126436
- Srinivasa, N., and Devi, T. P. (2014). Separation and identification of antifungal compounds from *Trichoderma* species BY GC-MS and their bio-efficacy against soil-borne pathogens. *BIOINFOLET- Jo. L. Sci.* 11, 255–257.
- Steddom, K., Heidel, G., Jones, D., and Rush, C. M. (2003). Remote detection of rhizomania in sugar beets. *Phytopathology* 93, 720–726. doi: 10.1094/PHYTO.2003.93.6.720
- Steyaert, J. M., Ridgway, H. J., Elad, Y., and Stewart, A. (2003). Genetic basis of mycoparasitism: a mechanism of biological control by species of *Trichoderma*. *New Zeal. J. Crop Hort. Sci.* 31, 281–291. doi: 10.1080/01140671.2003.9514263
- Subbarao, K. V. (1998). Progress toward integrated management of lettuce drop. *Plant Dis.* 82, 1068–1078. doi: 10.1094/PDIS.1998.82.10.1068
- Subbarao, K. V., Davis, R. M., Gilbertson, R. L., and Raid, R. N. (eds.). (2017). *Compendium of Lettuce Diseases and Pests*. St. Paul, MN: APS Press, The American Phytopathological Society.
- Susić, N., Žibrat, U., Sinkovič, L., Vončina, A., Razinger, J., Knapič, M., et al. (2020). From genome to field—observation of the multimodal nematocidal and plant growth-promoting effects of *Bacillus firmus* I-1582 on tomatoes using hyperspectral remote sensing. *Plants* 9:592. doi: 10.3390/plants9050592

- Thenkabail, P. S., Smith, R. B., and De Pauw, E. (2000). Hyperspectral vegetation indices and their relationships with agricultural crop characteristics. *Rem. Sens. Environ.* 71, 158–182. doi: 10.1016/S0034-4257(99)00067-X
- Thomas, S., Kuska, M. T., Bohnenkamp, D., Brugger, A., Alisaac, E., Wahabzada, M., et al. (2018). Benefits of hyperspectral imaging for plant disease detection and plant protection: a technical perspective. *J. Plant Dis. Protect.* 125, 5–20. doi: 10.1007/s41348-017-0124-6
- Thompson, J. D., Higgins, D. G., and Gibson, T. J. (1994). CLUSTAL W: improving the sensitivity of progressive multiple sequence alignment through sequence weighting, position-specific gap penalties and weight matrix choice. *Nucleic Acids Res.* 22, 4673–4680. doi: 10.1093/nar/22.22.4673
- Tian, Y. C., Yao, X., Yang, J., Cao, W. X., Hannaway, D. B., and Zhu, Y. (2011). Assessing newly developed and published vegetation indices for estimating rice leaf nitrogen concentration with ground- and space-based hyperspectral reflectance. *Field Crops Res.* 120, 299–310. doi: 10.1016/j.fcr.2010.11.002
- Tilley, D. R., Ahmed, M., Son, J. H., and Badrinarayanan, H. (2003). Hyperspectral reflectance of emergent macrophytes as an indicator of water column ammonia in an oligohaline, subtropical marsh. *Ecol. Eng.* 21, 153–163. doi: 10.1016/j.ecoleng.2003.10.004
- Tucker, C. J. (1979). Red and photographic infrared linear combinations for monitoring vegetation. *Remote Sens. Environ.* 8, 127–150. doi: 10.1016/0034-4257(79)90013-0
- Turner, G. J., and Tribe, H. T. (1976). On *Coniothyrium minitans* and its parasitism of *Sclerotinia* species. *Trans. Brit. Mycol. Soc.* 66, 97–105. doi: 10.1016/S0007-1536(76)80098-8
- Vitorino, L. C., Silva, F. O., da, Cruvinel, B. G., Bessa, L. A., Rosa, M., Souchie, E. L., et al. (2020). Biocontrol potential of *Sclerotinia sclerotiorum* and physiological changes in soybean in response to *Butia archeri* palm rhizobacteria. *Plants* 9:64. doi: 10.3390/plants9010064
- Vogelmann, J. E., Rock, B. N., and Moss, D. M. (1993). Red edge spectral measurements from sugar maple leaves. *Int. J. Remote Sens.* 14, 1563–1575. doi: 10.1080/01431169308953986
- Wang, Z., Li, Y., Zhuang, L., Yu, Y., Liu, J., Zhang, L., et al. (2019). A rhizosphere-derived consortium of *Bacillus subtilis* and *Trichoderma harzianum* suppresses common scab of potato and increases yield. *Comput. Struct. Biotechnol. J.* 17, 645–653. doi: 10.1016/j.csbj.2019.05.003
- Whipps, J. M., and Budge, S. P. (1990). Screening for sclerotial mycoparasites of *Sclerotinia sclerotiorum*. *Mycol. Res.* 94, 607–612. doi: 10.1016/S0953-7562(09)80660-6
- White, T. J., Burns, T., Lee, S., and Taylor, J. (1990). “Amplification and sequencing of fungal ribosomal RNA genes for phylogenetics,” in *PCR Protocols A Guide to Methods and Applications*, eds M. A. Innis, D. H. Gelfand, J. J. Sninsky, and T. J. White (San Diego, CA: Academic Press), 315–322.
- Wiegand, C. L., and Hatfield, J. L. (1988). “The spectral-agronomic multisite-multicrop analyses (SAMMA) project,” in *Proceedings of the 16th International Society for Photogrammetry and Remote Sensing Congress* (Kyoto), 696–706
- Wonglom, P., Daengsuwan, W., Ito, S., and Sunpapao, A. (2019). Biological control of *Sclerotium* fruit rot of snake fruit and stem rot of lettuce by *Trichoderma* sp. T76-12/2 and the mechanisms involved. *Physiol. Mol. Plant Pathol.* 107, 1–7. doi: 10.1016/j.pmp.2019.04.007
- Wu, C., Niu, Z., Tang, Q., and Huang, W. (2008). Estimating chlorophyll content from hyperspectral vegetation indices: modeling and validation. *Agr. Forest Meteorol.* 148, 1230–1241. doi: 10.1016/j.agrformet.2008.03.005
- Xing, N., Huang, W., Xie, Q., Shi, Y., Ye, H., Dong, Y., et al. (2020). A transformed triangular vegetation index for estimating winter wheat leaf area index. *Remote Sens.* 12:16. doi: 10.3390/rs12010016
- Xue, J., and Su, B. (2017). Significant remote sensing vegetation indices: a review of developments and applications. *J. Sens.* 2017, 1–17. doi: 10.1155/2017/1353691
- Yang, D., Wang, B., Wang, J., Chen, Y., and Zhou, M. (2009). Activity and efficacy of *Bacillus subtilis* strain NJ-18 against rice sheath blight and sclerotinia stem rot of rape. *Biol. Control.* 51, 61–65. doi: 10.1016/j.biocontrol.2009.05.021
- Yao, H., Tang, L., Tian, L., Brown, R. L., Bhatnagar, D., and Cleveland, T. E. (2011). “Using hyperspectral data in precision farming applications,” in *Hyperspectral Remote Sensing of Vegetation*, eds P. S. Thenkabail, and J. G. Lyon (Boca Raton, FL; London; New York, NY: CRC Press/Taylor and Francis Group), 591–608.
- Zarco-Tejada, P. J., Berjón, A., López-Lozano, R., Miller, J. R., Martín, P., Cachorro, V., et al. (2005). Assessing vineyard condition with hyperspectral indices: leaf and canopy reflectance simulation in a row-structured discontinuous canopy. *Remote Sens. Environ.* 99, 271–287. doi: 10.1016/j.rse.2005.09.002
- Zarco-Tejada, P. J., Miller, J. R., Noland, T. L., Mohammed, G. H., and Sampson, P. H. (2001). Scaling-up and model inversion methods with narrowband optical indices for chlorophyll content estimation in closed forest canopies with hyperspectral data. *IEEE Trans. Geosci. Remote Sens.* 39, 1491–1507. doi: 10.1109/36.934080
- Zhao, H., Yang, C., Guo, W., Zhang, L., and Zhang, D. (2020). Automatic estimation of crop disease severity levels based on vegetation index normalization. *Remote Sens.* 12:1930. doi: 10.3390/rs12121930

Conflict of Interest: The authors declare that the research was conducted in the absence of any commercial or financial relationships that could be construed as a potential conflict of interest.

Copyright © 2021 Manganiello, Nicastro, Caputo, Zaccardelli, Cardi and Pane. This is an open-access article distributed under the terms of the Creative Commons Attribution License (CC BY). The use, distribution or reproduction in other forums is permitted, provided the original author(s) and the copyright owner(s) are credited and that the original publication in this journal is cited, in accordance with accepted academic practice. No use, distribution or reproduction is permitted which does not comply with these terms.